The Elastic Rod Model for DNA and Its Application to the Tertiary Structure of DNA Minicircles in Mononucleosomes

David Swigon,* Bernard D. Coleman,* and Irwin Tobias#
*Department of Mechanics and Materials Science and #Department of Chemistry, Rutgers, The State University of New Jersey, Piscataway, New Jersey 08854 USA

ABSTRACT Explicit solutions to the equations of equilibrium in the theory of the elastic rod model for DNA are employed to develop a procedure for finding the configuration that minimizes the elastic energy of a minicircle in a mononucleosome with specified values of the minicircle size N in base pairs, the extent w of wrapping of DNA about the histone core particle, the helical repeat h_0^b of the bound DNA, and the linking number L_k of the minicircle. The procedure permits a determination of the set $\mathcal{S}(N, w, h_0^b)$ of integral values of L_k for which the minimum energy configuration does not involve self-contact, and graphs of writhe versus w are presented for such values of L_k. For the range of N of interest here, $330 < N < 370$, the set $\mathcal{S}(N, w, h_0^b)$ is of primary importance: when L_k is not in $\mathcal{S}(N, w, h_0^b)$, the configurations compatible with L_k have elastic energies high enough to preclude the occurrence of an observable concentration of topoisomer L_k in an equilibrium distribution of topoisomers. Equilibrium distributions of L_k, calculated by setting differences in the free energy of the extranucleosomal loop equal to differences in equilibrium elastic energy, are found to be very close to Gaussian when computed under the assumption that w is fixed, but far from Gaussian when it is assumed that w fluctuates between two values. The theoretical results given suggest a method by which one may calculate DNA-histone binding energies from measured equilibrium distributions of L_k.

INTRODUCTION

The research reported here is part of an ongoing effort toward the attainment of insight into the relation between the tertiary structure of a segment of duplex DNA and geometric conditions imposed at the end points of the segment. In this research we employ the elastic rod model for DNA and hence specify the configuration of a DNA molecule by giving its duplex axis and the rate of twisting of one of the two DNA strands about that axis. The use of explicit and exact solutions to the equations of mechanical equilibrium for elastic rods can greatly simplify the problem of calculating the dependence of the configuration and elastic energy of an otherwise free segment of duplex DNA on geometric conditions imposed at its end points (cf. Tobias et al., 1994; Coleman et al., 1995). This method of exact solutions is appropriate to cases in which the segment is intrinsically straight, i.e., is such that its axis is straight in the stress-free state. We here apply the method to the extranucleosomal loop $\mathcal{R}^f$ in a small DNA plasmid, called a *minicircle*, that has formed a mononucleosome with a histone core particle (see Fig. 1 below). The equilibrium configurations of $\mathcal{R}^f$ depend on the following parameters: (1) the number N of base pairs in the minicircle, (2) the amount w of wrapping of DNA around the histone core particle (called the *wrap*), (3) the twist-related helical repeat h_0^b of that part of nucleosomal DNA that is tightly bound to the core particle, and (4) the linking number L_k of the minicircle. Our analysis of configurations of $\mathcal{R}^f$ enables us to develop a procedure for finding a configuration that minimizes the elastic energy of the minicircle when these four parameters have been specified, and we employ that procedure to derive properties of equilibrium distributions of topoisomers in mononucleosomes.

As the parameters N, w, h_0^b, and L_k suffice to determine a minimum energy configuration of the minicircle, in formulating the elastic elastic rod model, we do not refer to such aspects of histone-DNA interactions as the relative importance of site-specific binding and long-range electrostatic forces, or the manner in which nucleotide sequences differ in their affinity for the octamer. However, as a change in the overall wrapping of DNA about the core particle results in a (positive or negative) increment in the free energy of the mononucleosome and this increment is the sum of two quantities, an increment in the configuration-dependent free energy of $\mathcal{R}^f$ (which our theory permits us to calculate) and an increment Γ in the total DNA-histone binding energy, the theory suggests a method by which one eventually may be able to obtain information about DNA-histone binding energies from measurements of equilibrium distributions of topoisomers. Several of the difficulties associated with the problem of relating the results of relaxation experiments to binding energies are discussed at the end of this introduction.

Our calculations are confined to cases in which N is in the range 330–370 bp, and the length of $\mathcal{R}^f$ is less than two persistence lengths (i.e., less than 282 bp). We make the assumption that the increment ΔG in the free energy of a mononucleosome due to a change in L_k from $L_k^{(A)}$ to $L_k^{(B)}$, with N, w, and h_0^b assumed constant, can be equated to the difference in the elastic energies of the minimum energy

Received for publication 7 August 1997 and in final form 5 January 1998.
Address reprint requests to Dr. Bernard D. Coleman, Department of Mechanics and Materials Science, Rutgers University, 98 Brett Rd., Room B134, Piscataway, NJ 08854-8058. Tel.: 732-445-5558; Fax: 732-445-0085; E-mail: bcoleman@stokes.rutgers.edu.

0006-3495/98/05/2515/16 $2.00

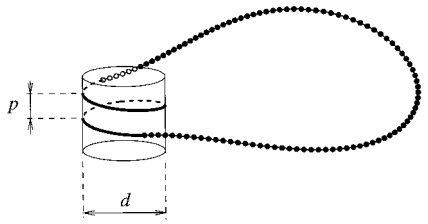

FIGURE 1 Schematic drawing of the axial curve $\mathscr{C}$ of a DNA minicircle $\mathscr{R}$ and the histone core particle. The core particle is shown as a cylinder. The axial curve $\mathscr{C}^{b}$ of $\mathscr{R}^{b}$, the nucleosomal part of $\mathscr{R}$, is drawn as a heavy curve that is solid in front of the core particle and dashed behind it. $\mathscr{C}^{f}$, the axial curve of the extranucleosomal loop, $\mathscr{R}^{f}$, is represented by a succession of circles that are open when behind the particle and solid otherwise. In the figure the relative lengths of $\mathscr{C}^{b}$ and $\mathscr{C}^{f}$ correspond to a minicircle of 359 bp that is wrapped about the core particle for 1.45 turns.

configurations corresponding to (N, w, h_0^b, $L_k^{(A)}$) and (N, w, h_0^b, $L_k^{(B)}$). This assumption, which appears appropriate for the range of N considered, is employed to develop a theory of the equilibrium topoisomer distributions obtained when minicircles in mononucleosomes are relaxed with, say, topoisomerase I. (Some justification for the assumption is provided by a paper (Tobias, 1998) on thermal fluctuations in protein-free DNA plasmids appearing in this issue of the *Biophysical Journal*. Expressions given in that paper imply that when a segment of DNA shorter than two persistence lengths is free along its length from external forces and moments, as is $\mathscr{R}^{f}$, and, in addition, has the form of a closed circle, the entropy contribution to the free energy of supercoiling is less than 11% of the elastic energy contribution.) Our assumption about ΔG differs from that made by Le Bret (1988), who used a Monte Carlo method to calculate average values of L_k for equilibrium mixtures of minicircles in mononucleosomes with w fixed. Le Bret's seminal paper, although based on a different approach to the problem, influenced the present research.

Our procedure for finding minimum energy configurations and calculating their properties (e.g., elastic energy, writhe) as functions of N, w, h_0^b, and L_k is explained in the next section of the paper. There we give figures showing such configurations for two values of N.

For given N, w, and h_0^b, our theory enables us to determine the set $\mathscr{S}(N, w, h_0^b)$ of integers L_k for which the minimum energy configuration is without self-contact. Graphs of writhe versus wrap are presented for values of L_k in $\mathscr{S}(N, w, h_0^b)$; the calculation of these graphs was facilitated by new results in the theory of rods that are presented in Appendix B (Eqs. B1 and B6–B12). In the range of N for which we do calculations, when $L_k^{\#}$ is a linking number not in $\mathscr{S}(N, w, h_0^b)$, the minimum energy configuration for the quadruple (N, w, h_0^b, $L_k^{\#}$) not only shows self-contact, but has an elastic energy $\Psi^{\#}$ that exceeds the elastic energy Ψ^{*} of the minimum energy configuration for each L_k in $\mathscr{S}(N, w, h_0^b)$ by an amount sufficient to preclude the occurrence of an observable concentration of topoisomer $L_k^{\#}$ in an equilibrium distribution of topoisomers.

Equilibrium distributions of topoisomers are discussed in the final section of the paper. We treat two mathematical cases. For the first, the case in which all of the nucleosomes are assumed to have the same wrap, we give expressions for the concentration of topoisomers with integral linking number L_k and present calculated graphs of the dependence on N of the average value of L_k. We show that the probability density function for the corresponding continuous distribution of L_k departs only slightly from a Gaussian probability density function characterized by two parameters, $\bar{L}_k$ and K, that can be calculated from first principles. The dependence of these parameters on h_0^b and N is discussed.

Once a theory of topoisomer distributions for mononucleosomes with a specified wrap is in hand, one can construct a more general theory in which transitions between various amounts of wrapping are possible. We do this for the simplest case, in which w is allowed two values, $w^{(1)}$ and $w^{(2)} > w^{(1)}$, and derive a formula (Eq. 41) giving the DNA-histone binding energy for the transition from $w^{(1)}$ to $w^{(2)}$ as a function of the ratio of equilibrium concentrations of two topoisomers. Our development of the two-state model shows that it can yield probability density functions for continuous distributions of L_k that are far from Gaussian and, in some cases, bimodal. For that model an expression is obtained relating the difference in binding energy $\Gamma(w^{(1)}, w^{(2)})$ for the two states of wrap to the ratio of equilibrium concentrations of any two distinct topoisomers.

For $N = 341$, 354, and 359 bp, Zivanovic et al. (1988) have published results of relaxation experiments for mononucleosomes. (For reasons discussed in the second section of the present paper, the published topoisomer distribution for $N = 354$ is not useful for our purposes.) When $N = 359$, a single topoisomer $L_k = 33$ predominates at equilibrium. When $N = 341$, our calculations indicate that the equilibrium mixture contains two topoisomers, $L_k = 31$ and $L_k = 32$, and from the experimentally measured ratio of their concentrations a value of Γ can be derived. We illustrate the way such a calculation proceeds, but we do not propose that one accept as definitive the value of Γ that we obtain. General principles in the theory of rods and recent Monte Carlo calculations of Katritch and Vologodskii (1997) for protein-free DNA plasmids suggest that equilibrium distributions of L_k can be sensitive to small departures from the assumption that the DNA is intrinsically straight, and we do not know how close to that assumption were the DNA fragments used to form the 341- and 359-bp minicircles of published experiments. (As those fragments were prepared by *Mbo*I cleavage of pBR322, which has a known nucleotide sequence (Sutcliffe, 1978, 1979; Watson, 1988), one can, in principle, calculate the detailed distribution of intrinsic curvature along the fragments, but we are not aware of that having been done.) Of course, even if it be shown that the minicircles studied are made of DNA that is close to intrinsically straight, in the comparison of theory and experiment there remain difficulties associated with uncer-

tainty in the assigned values of $w^{(1)}$, $w^{(2)}$, and h_0^b, the present lack of data for other values of N, and the possibility that the two-state model is an oversimplification of a more appropriate multistate model.

The emphasis in this paper is on the theory of the elastic rod model and the development of methods for its eventual application to DNA-protein interactions, not on numerical results for specific experiments. We find that a two-state model for fluctuations in w can yield topoisomer distributions that differ not only quantitatively but also qualitatively from the nearly Gaussian distributions implied by a model in which w is fixed. One can construct other hypothetical models for fluctuations in the extent of binding of DNA to the histone octamer, and we expect that the methods presented here can be used to search for distinguishing qualitative characteristics of their implications.

CONFIGURATIONS AND ELASTIC ENERGY

As in earlier studies in which the elastic rod model is employed for a plasmid in a mononucleosome (e.g., Le Bret, 1988; Zhang et al., 1994), a DNA molecule here is represented by an inextensible, homogeneous, transversely isotropic, intrinsically straight rod $\mathcal{R}$ whose axial curve $\mathcal{C}$ is the curve in space occupied by the duplex axis. This curve is described by giving the radial vector $\boldsymbol{r}$ from an origin $\mathbf{O}$ to a point on $\mathcal{C}$ as a function of arc-length s. For a closed DNA minicircle of length Λ that is wrapped about a histone core to form a mononucleosome, $\mathcal{R}$ is a closed rod made up of (1) nucleosomal DNA, i.e., a bound segment $\mathcal{R}^b$ with axial curve $\mathcal{C}^b$ and length Λ^b, which is in contact with the core particle; and (2) the free segment $\mathcal{R}^f$ (or extranucleosomal loop) with axial curve $\mathcal{C}^f$ and length $\Lambda^f = \Lambda - \Lambda^b$. (In this paper lengths that are denoted by the symbols Λ, Λ^f, Λ^b when measured in nanometers are denoted by N, N^f, N^b when measured in base pairs (with 1 bp = 0.34 nm).)

We consider the case in which the core particle is the histone octamer formed from the histone proteins H2A, H2B, H3, and H4, and the linker histone H1 is not present, as was the case for the mononucleosomes of experiments of Zivanovic et al. (1988) that we shall discuss later in the paper. In accord with currently available structural information (Richmond et al., 1984; Arents and Moudrianakis, 1993), we suppose that $\mathcal{C}^b$ is, as in Fig. 1, a left-handed helix with a pitch p of 2.7 nm and a diameter d of 8.6 nm.

(*Note added after submission of the paper*: A recently published announcement of the x-ray structure of the nucleosome core at 0.28-nm resolution (Luger et al., 1997) gives values of 2.39 nm for p and 8.36 nm for d in the optimal helical approximation to the duplex axis of the nucleosomal DNA. Our recent calculations indicate that the reduction in the values of p and d called for by the new structural data will not have a major effect on the results reported here.)

The amount, in turns, that $\mathcal{C}^b$ is wrapped about the core particle (i.e., the wrap) is denoted by w. The assumption that $\mathcal{C}^b$ is a helix yields

$$\Lambda^b = w\sqrt{\pi^2 d^2 + p^2}. \tag{1}$$

The configuration of $\mathcal{R}^f$ is calculated using Kirchhoff's theory of elastic rods (Kirchhoff, 1859, 1876; Dill, 1992) and boundary conditions that follow from the assumption that both $\boldsymbol{r}(s)$ and $\boldsymbol{t}(s) = \boldsymbol{r}'(s) = \mathrm{d}\mathbf{r}(s)/\mathrm{d}s$ are continuous for all values of s, including the two, s_A, s_B, characterizing the places where $\mathcal{R}^b$ and $\mathcal{R}^f$ meet. Of the various configurations for $\mathcal{R}^f$ that are compatible with this assumption and preassigned values of the wrap and the linking number of $\mathcal{R}$, we select the one that minimizes elastic energy.

We write L_k for the linking number of the DNA minicircle $\mathcal{R}$, i.e., the number of times the duplex axis $\mathcal{C}$ is linked with either one of the DNA strands of the minicircle. (The topologically invariant integer L_k was introduced by Gauss and is discussed in several modern texts, among them that of Courant (1936); see also Calugareanu (1961).) By a now familiar result (White, 1969), the topological constant L_k is the sum of the twist T_w of either DNA strand about the duplex axis and the writhe W_r of that axis:

$$L_k = T_w + W_r. \tag{2}$$

For a DNA molecule of length Λ, whether open or closed,

$$T_w = \frac{1}{2\pi}\int_0^\Lambda \Omega(s)\mathrm{d}s, \tag{3}$$

where Ω, the twist density, is the rate of wrapping of either strand about the duplex axis and is expressed in units of radians per unit length. When the molecule is in a straight stress-free configuration, Ω equals $\Omega_0 = 2\pi/(0.34h_0)$, the intrinsic twist density of duplex DNA. The number h_0, which depends on the temperature T, the solvent composition, and the nucleotide sequence, is the helical repeat of stress-free DNA. The writhe W_r of the closed curve $\mathcal{C}$ is given by the double integral

$$W_r = \frac{1}{4\pi}\int_0^\Lambda\int_0^\Lambda \frac{\boldsymbol{t}(s)\times\boldsymbol{t}(s^*)\cdot[\boldsymbol{r}(s)-\boldsymbol{r}(s^*)]}{|\boldsymbol{r}(s)-\boldsymbol{r}(s^*)|^3}\,\mathrm{d}s\,\mathrm{d}s^* \tag{4}$$

and equals the number obtained by averaging, over all orientations of a plane $\mathcal{P}$, the sum of the signed self-crossings occurring in the planar curves resulting from perpendicular projection of $\mathcal{C}$ on $\mathcal{P}$ (Fuller, 1971). In Appendix B we describe our method of evaluating W_r and show that exact solutions we obtain for $\mathcal{C}^f$, and hence $\mathcal{C}$, yield essentially explicit expressions for W_r.

A configuration $\mathcal{X}$ (or mechanical state) of a rod is specified by giving the axial curve of the rod and the twist density $\Omega(s)$ along that curve.

We first discuss $\mathcal{R}^b$. As the axial curve $\mathcal{C}^b$ of $\mathcal{R}^b$ obeys the assumptions stated above Eq. 1, once we have assigned a value to the wrap w, not only the length Λ^b of $\mathcal{C}^b$, but $\mathcal{C}^b$

itself will be specified, and the configuration of $\mathcal{R}^b$ will be determined when the twist density $\Omega(s)$ is given along $\mathcal{C}^b$. Recent measurements of Hamiche and Prunell (1992) of the dependence on N and T of the average twist density of DNA minicircles in mononucleosomes are compatible with the assumptions that (1) a subsegment $\mathcal{R}_0^b$ of $\mathcal{R}^b$, with a length N_0^b that they found to be 109 ± 25 bp, has a twist density Ω_0^b that appears to be independent not only of N and L_k, but also of T; and (2) when $\mathcal{R}_0^b$ is not all of $\mathcal{R}^b$, the remaining bound DNA, of length $N^b - N_0^b$, is in torsional equilibrium with $\mathcal{R}^f$. It is natural to assume that when N^b exceeds N_0^b, the segment $\mathcal{R}_0^b$ is centrally located in $\mathcal{R}^b$, which implies that one can regard the bound segment $\mathcal{R}^b$ as a union of three abutting segments, $\mathcal{R}_-^b$, $\mathcal{R}_0^b$, and $\mathcal{R}_+^b$, with the two outer segments, $\mathcal{R}_-^b$ and $\mathcal{R}_+^b$, of equal length, $(N^b - N_0^b)/2$. For the total twist of $\mathcal{R}_0^b$ we have

$$T_w^{b,0} = \frac{1}{2\pi}\Lambda_0^b\Omega_0^b = N_0^b/h_0^b; \tag{5}$$

h_0^b is the twist-related helical repeat of the central segment of the nucleosomal DNA. We shall present results concerning the influence of h_0^b on equilibrium distributions of topoisomers with fixed values of w.

The crystal structure determination of Richmond et al. (1984) indicates that the maximum value of w is in the range 1.7 to 1.8. In the calculations to be presented, two values of w are emphasized: 1.70 turns and an alternative value of 1.45 turns, which is not far from an average of values observed by electron microscopy for minicircles in mononucleosomes in aqueous media at low ionic strength (Zivanovic et al., 1988). It is not only convenient for us, but also in accord with the range of observations of Hamiche and Prunell (1992), to assume that the length of $\mathcal{R}_0^b$ corresponds to $w = 1.45$ turns. Then the DNA that is added to the core particle when w is increased from 1.45 to 1.70 turns constitutes the two outer segments, $\mathcal{R}_-^b$, $\mathcal{R}_+^b$, that one expects to be more loosely bound than the central segment.

Our calculations of configurations and elastic energies of mononucleosomes give results that are not sensitive to the assumed length of $\mathcal{R}_0^b$, throughout the range compatible with the data of Hamiche and Prunell (1992). As we have no information about the values of torsional rigidity C and intrinsic twist density Ω_0 for $\mathcal{R}_-^b$ and $\mathcal{R}_+^b$, we assume that C and Ω_0 are the same for those two segments as for the free segment $\mathcal{R}^f$. Hindsight has shown that calculated values of elastic energies would have differed by no more than 1% from those that we shall report here, if we had assumed that even when $w = 1.70$, all of the bound DNA has a fixed twist density $\Omega_0^b = 2\pi/(0.34h_0^b)$. In other words, by allowing for the possibility that there are two outer segments, $\mathcal{R}_-^b$, $\mathcal{R}_+^b$, that have properties different from those of $\mathcal{R}_0^b$, we have introduced a small complication that does not appear to have been necessary. As the emphasis here is on methods, however, we have chosen to describe our model at a level of generality that may be useful if subsequent experiments show in a convincing way that the length of $\mathcal{R}_0^b$ should be taken to be significantly less than the one we have employed.

For a given total length Λ and linking number L_k, once the wrap w is specified, the assumptions just stated about the bound segment $\mathcal{R}^b$ can be combined with solutions in the theory of the elastic rod model to find an appropriate equilibrium configuration of $\mathcal{R}^f$ under the assumption that the only external forces and moments acting on $\mathcal{R}^f$ or any subsegment of $\mathcal{R}^f$ are those applied at the segment's end points. When this assumption, which implies that $\mathcal{R}^f$ is free from self-contact, is granted, the laws of balance of forces and moments, as expressed in the theory of rods, reduce to the assertion that the resultant $\boldsymbol{F} = \boldsymbol{F}(s)$ of the internal stresses on a cross section of $\mathcal{R}^f$ and the net moment $\boldsymbol{M} = \boldsymbol{M}(s)$ of those internal stresses obey the equations

$$\boldsymbol{F}' = \boldsymbol{0}, \tag{6}$$

$$\boldsymbol{M}' = \boldsymbol{F} \times \boldsymbol{t}. \tag{7}$$

When the minicircle under consideration, and hence $\mathcal{R}^f$, is formed from intrinsically straight DNA that is homogeneous in its mechanical properties, Kirchhoff's constitutive equation for $\boldsymbol{M}$ yields

$$\boldsymbol{M} = A(\boldsymbol{t} \times \boldsymbol{t}') + C\Delta\Omega^f\boldsymbol{t}, \qquad \Delta\Omega^f = \Omega^f - \Omega_0, \tag{8}$$

where the coefficients of flexural rigidity A and torsional rigidity C are constants, and Ω^f is the twist density present in $\mathcal{R}^f$. The system of equations obtained by combining Eqs. 6, 7, and 8 will here be called Kirchhoff's equations of equilibrium. By Eq. 8, $\boldsymbol{M} \cdot \boldsymbol{t} = C\,\Delta\Omega^f$, and hence Eq. 7 implies that the excess twist density, $\Delta\Omega^f$, is constant along $\mathcal{R}^f$ and hence on $\mathcal{R}_+^b \cup \mathcal{R}^f \cup \mathcal{R}_-^b$. In view of Eqs. 3 and 5, the total twist T_w of $\mathcal{R}$ is

$$T_w = \frac{N_0^b}{h_0^b} + \frac{1}{2\pi}(\Lambda - \Lambda_0^b)\Omega^f. \tag{9}$$

We now discuss the problem of finding, for given values of the quadruple (Λ, w, h_0^b, L_k), the configuration $\mathcal{Z}^*$ of $\mathcal{R}$ that satisfies the following four conditions: (I) Kirchhoff's equations of equilibrium hold on $\mathcal{R}^f$, and hence $\mathcal{R}$ is free from self-contact; (II) Eqs. 3 and 4 yield values of T_w and W_r for $\mathcal{R}$ with $T_w + W_r$ equal to the given value of L_k; (III) $\boldsymbol{r}(s)$ and $\boldsymbol{t}(s)$ are continuous at the places where $\mathcal{R}^b$ and $\mathcal{R}^f$ meet; and (IV) of all configurations compatible with (I)–(IV) and the specified quadruple (Λ, w, h_0^b, L_k), $\mathcal{Z}^*$ gives the smallest value to the energy Ψ, defined as the sum

$$\Psi = \Psi^f + \Psi_+^b + \Psi_-^b, \tag{10}$$

in which

$$\Psi^f = \frac{1}{2}\int_{\mathcal{C}^f}[A\kappa^2 + C(\Omega - \Omega_0)^2]\mathrm{d}s, \tag{11}$$

(with κ the geometric curvature of $\mathcal{C}^f$) is the elastic energy of the free segment $\mathcal{R}^f$, and Ψ_+^b and Ψ_-^b are the twist energies of the segments $\mathcal{R}_-^b$ and $\mathcal{R}_+^b$.

We note that in a state of mechanical equilibrium,

$$\Psi^{\mathrm{b}}_{+} = \Psi^{\mathrm{b}}_{-} = \frac{C}{4}(\Lambda^{\mathrm{b}} - \Lambda^{\mathrm{b}}_0)(\Delta\Omega^{\mathrm{f}})^2, \tag{12}$$

and Ψ in Eq. 10 is given by

$$\Psi = \frac{A}{2}\int_{\mathscr{C}^{\mathrm{f}}} \kappa^2 \, \mathrm{d}s + \frac{C}{2}(\Lambda - \Lambda^{\mathrm{b}}_0)(\Delta\Omega^{\mathrm{f}})^2. \tag{13}$$

A method is available for finding exact and explicit solutions of Eqs. 6, 7, and 8 for specified values of $\boldsymbol{r}(s_{\mathrm{A}})$, $\boldsymbol{t}(s_{\mathrm{A}})$, $\boldsymbol{r}(s_{\mathrm{B}})$, $\boldsymbol{t}(s_{\mathrm{B}})$, Λ^{f}, and $\Delta\Omega^{\mathrm{f}}$ (Tobias et al., 1994; Coleman et al., 1995). The method is explained and applied to the present problem in Appendix A. There we make use of geometric relations between the triples (p, d, w) and $(\boldsymbol{r}(s_{\mathrm{A}}) - \boldsymbol{r}(s_{\mathrm{B}}), \boldsymbol{t}(s_{\mathrm{A}}), \boldsymbol{t}(s_{\mathrm{B}}))$ to obtain a procedure for calculating, for given values of Λ and w, the dependence on $\Delta\Omega^{\mathrm{f}}$ of the curve $\mathscr{C}^{\mathrm{f}}$ and hence of W_{r}, which gives us the function $\tilde{W}_{\mathrm{r}}$ in the relation

$$W_{\mathrm{r}} = \tilde{W}_{\mathrm{r}}(\Delta\Omega^{\mathrm{f}}; \Lambda, w), \tag{14}$$

and, in view of Eqs. 2 and 9, yields L_{k} as a function of $\Delta\Omega^{\mathrm{f}}$:

$$L_{\mathrm{k}} = \tilde{W}_{\mathrm{r}}(\Delta\Omega^{\mathrm{f}}; \Lambda, w) + \frac{N^{\mathrm{b}}_0}{h^{\mathrm{b}}_0} + \frac{1}{2\pi}(\Lambda - \Lambda^{\mathrm{b}}_0)(\Delta\Omega^{\mathrm{f}} + \Omega_0). \tag{15}$$

We can invert this function to obtain $\Delta\Omega^{\mathrm{f}}$ as a function of L_{k}. As the parameters Λ^{b}_0 and Ω_0 are fixed throughout our discussion, we are thus able to find the configurations $\mathscr{Z}$ of the minicircle that correspond to a specified quadruple $(\Lambda, w, h^{\mathrm{b}}_0, L_{\mathrm{k}})$ and obey the conditions (I)–(III). These configurations $\mathscr{Z}$ form a set $\mathscr{A}(\Lambda, w, h^{\mathrm{b}}_0, L_{\mathrm{k}})$ that need not be finite. Of interest to us is $\mathscr{Z}^*(\Lambda, w, h^{\mathrm{b}}_0, L_{\mathrm{k}})$, the configuration in $\mathscr{A}(\Lambda, w, h^{\mathrm{b}}_0, L_{\mathrm{k}})$ that obeys the condition (IV), i.e., that minimizes the elastic energy Ψ in Eq. 13 over $\mathscr{A}(\Lambda, w, h^{\mathrm{b}}_0, L_{\mathrm{k}})$. If $\mathscr{A}(\Lambda, w, h^{\mathrm{b}}_0, L_{\mathrm{k}})$ is not empty, $\mathscr{Z}^*(\Lambda, w, h^{\mathrm{b}}_0, L_{\mathrm{k}})$ exists and is free from self-contact.

As we observe in Appendix A, the method of exact solutions yields an elementary formula (Eq. A18) for the elastic energy Ψ^{f} of Eq. 11 as a function of parameters that can be related to Λ, w, and $\Delta\Omega^{\mathrm{f}}$ and that uniquely characterize each configuration in $\mathscr{A}(\Lambda, w, h^{\mathrm{b}}_0, L_{\mathrm{k}})$. Use of that formula greatly facilitates the solution of the problem of finding the minimizer $\mathscr{Z}^*$ of Ψ over $\mathscr{A}$. It also permits one to evaluate Ψ as a function $\tilde{\Psi}$of $\Delta\Omega^{\mathrm{f}}$ for fixed Λ and w, i.e.,

$$\Psi = \tilde{\Psi}(\Delta\Omega^{\mathrm{f}}; \Lambda, w), \tag{16}$$

which is a matter of importance for a discussion of the dependence of Ψ on h^{b}_0 to be presented in the following section.

Suppose the triple $(\Lambda, w, h^{\mathrm{b}}_0)$ has been specified, and let $\mathscr{S}(\Lambda, w, h^{\mathrm{b}}_0)$ or $\mathscr{S}(N, w, h^{\mathrm{b}}_0)$ be the set of integers L_{k} such that the configuration $\mathscr{Z}^*(\Lambda, w, h^{\mathrm{b}}_0, L_{\mathrm{k}})$, i.e., the configuration that obeys the conditions (I)–(IV), gives a global minimum to Ψ in Eq. 10 over the set $\mathscr{B}(\Lambda, w, h^{\mathrm{b}}_0, L_{\mathrm{k}})$ of all configurations with the indicated value of the quadruple $(\Lambda, w, h^{\mathrm{b}}_0, L_{\mathrm{k}})$ that obey the conditions (II) and (III), without regard to whether these configurations are in mechanical equilibrium or are free from self-contact. For short, we refer to $\mathscr{Z}^*$ as the "minimum energy configuration." For the value of Ψ at $\mathscr{Z}^*(\Lambda, w, h^{\mathrm{b}}_0, L_{\mathrm{k}})$, we write

$$\Psi = \Psi^*_{\Lambda, w, h^{\mathrm{b}}_0}(L_{\mathrm{k}}). \tag{17}$$

For L_{k} not in $\mathscr{S}(\Lambda, w, h^{\mathrm{b}}_0)$, let $\mathscr{Z}^{\#}$ be the configuration that minimizes Ψ over the set $\mathscr{B}(\Lambda, w, h^{\mathrm{b}}_0, L_{\mathrm{k}})$. The configuration $\mathscr{Z}^{\#}$ obeys the conditions (II)–(IV), but not condition (I), and hence is not free from self-contact. Thus $\mathscr{Z}^{\#}$ cannot be found by using the procedure described above. The authors recently have extended the method of exact solutions to obtain a procedure for calculating minimum energy configurations when points of self-contact are present, and in yet unpublished research have verified that, for the range of the parameters (N, w, h^{b}_0) for which results are reported in this paper, when L_{k} is not in $\mathscr{S}(N, w, h^{\mathrm{b}}_0)$, the equilibrium configurations compatible with L_{k} have elastic energies high enough to preclude the occurrence of L_{k} at an observable concentration in an equilibrium distribution of topoisomers.

When N_{f} is of the order of magnitude of a persistence length, for values of L_{k} in $\mathscr{S}(N, w, h^{\mathrm{b}}_0)$ the configuration $\mathscr{Z}^*(N, w, h^{\mathrm{b}}_0, L_{\mathrm{k}})$ may be considered thermodynamically stable in the sense that it minimizes the free energy G over the set $\mathscr{B}(N, w, h^{\mathrm{b}}_0, L_{\mathrm{k}})$. All of the calculations that we give in this paper are for minimum energy configurations $\mathscr{Z}^*$. The ranges of parameters (N, w, h^{b}_0) that we have investigated have been selected for their possible application to the interpretation of experimental results for mononucleosomes formed from minicircles with 330–370 bp, and in each case the set $\mathscr{S}(N, w, h^{\mathrm{b}}_0)$ was found to contain two elements.

For the calculations reported in this paper, we have chosen a value of A that corresponds to a persistence length A/RT of 50.0 nm at $T = 298$ K (cf. Hagerman, 1988), and we have assumed that C/A has a value 1.4, which is compatible with the results of relaxation experiments on protein-free DNA plasmids (Horowitz and Wang, 1984). To h_0 we have assigned a value of 10.53 bp/turn that Zivanovic et al. (1988) (see also Goulet et al., 1988) reported to be appropriate for their relaxation experiments on minicircles in mononucleosomes that were conducted at $T = 310$ K in a medium with an ionic strength of 125 mM.

Figs. 2 and 3 show minimum energy configurations for $N = 341$ and 359, when $w = 1.45$ and 1.70. Table 1 contains the corresponding computed values of the writhe W_{r}, the elastic energy $\Psi^*_{\Lambda, w, h^{\mathrm{b}}_0}(L_{\mathrm{k}})$, and the distance Δ of closest approach of the axial curve $\mathscr{C}^{\mathrm{f}}$ to itself. For these figures the twist-related helical repeat h^{b}_0 of the tightly bound segment $\mathscr{R}^{\mathrm{b}}_0$ was chosen to be 10.40 bp/turn, a value not far from the average of two proposed values: (1) 10.53 bp/turn, which is identical to h_0; and (2) 10.31 bp/turn, which corresponds (under the assumption that the core particle surface is truly cylindrical) to a value of 10.18 bp/turn for the cleavage periodicity measured by nuclease

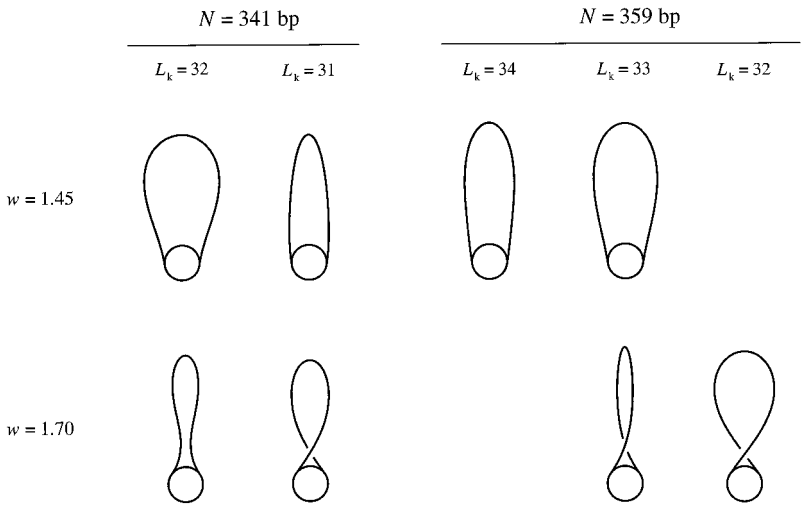

FIGURE 2 Calculated axial curves $\mathscr{C}$ for minimum energy configurations. The line of view is parallel to the axis of the core particle, and h_0^b is chosen to be 10.40 bp/turn.

digestion (Prunell et al., 1979; Lutter, 1979; Prunell, 1983) and hydroxyl radical cleavage (Hayes et al., 1990, 1991). Although calculated values of experimentally measurable quantities dependent on elastic energy can be sensitive to changes in h_0^b, expressions can be derived for the dependence of such quantities on h_0^b, once their values are known as functions of L_k for a single value of h_0^b; results of this type will be presented later in the paper.

The distance of closest approach, Δ, tells us how near to each other come sequentially separated segments of a DNA molecule. When $w = 1.45$ and $N = 341$ or 359, for each L_k in $\mathcal{S}(N, w, 10.40)$, the minimum value of $|\boldsymbol{r}(s_1) - \boldsymbol{r}(s_2)|$ for sequentially separated points s_1 and s_2 occurs when s_1 and s_2 are the end points s_A and s_B of $\mathcal{R}^f$, and hence $\Delta = |\boldsymbol{r}(s_A) - \boldsymbol{r}(s_B)|$. On the other hand, for the corresponding cases with $w = 1.70$, Δ is smaller than $|\boldsymbol{r}(s_A) - \boldsymbol{r}(s_B)|$. The smallest value of Δ in Table 1, namely 2.5 nm, corresponds to $N = 341$, $w = 1.70$, $L_k = 32$.

To characterize configurations that are "free from self-contact," we have followed a common practice and modeled steric effects by considering a DNA molecule to be a tube of diameter 2.0 nm. In this sense, the minimum energy configuration $\mathcal{L}^*(341, 1.70, 10.40, 32)$ is free from self-contact, and $L_k = 32$ is a valid member of the set $\mathcal{S}(341, 1.70, 10.40)$. However, at the low salt concentrations that are employed in relaxation experiments on mononucleosomes, electrostatic repulsion would cause the minimum energy configuration to differ from $\mathcal{L}^*$ and have a free energy that is significantly larger than an estimate based on only the elastic energy $\Psi^*_{\Lambda,w,h_0^b}(L_k)$.

Zivanovic et al. (1988) observed that relaxation of mononucleosomes with $N = 341$ yields topoisomers with $L_k = 31$ and 32. We find that these values of L_k are in both $\mathcal{S}(341, 1.45, 10.40)$ and $\mathcal{S}(341, 1.70, 10.40)$ and are the only values of L_k in those sets. The same experimenters observed that gel electrophoresis indicates that the product of relaxation of mononucleosomes with $N = 359$ is the topoisomer with $L_k = 33$, and only traces of others are present. For $N = 359$, we find that, in addition to the value 33 of L_k, $\mathcal{S}(359, 1.45, 10.40)$ contains the value 34, and $\mathcal{S}(359, 1.70, 10.40)$ contains the value 32. For $N = 359$, when $w = 1.45$, $\Psi^*(L_k = 34) > \Psi^*(L_k = 33) + 3$ kcal/mol, and when $w = 1.70$, $\Psi^*(L_k = 32) > \Psi^*(L_k = 33) + 1.5$ kcal/mol, and hence the

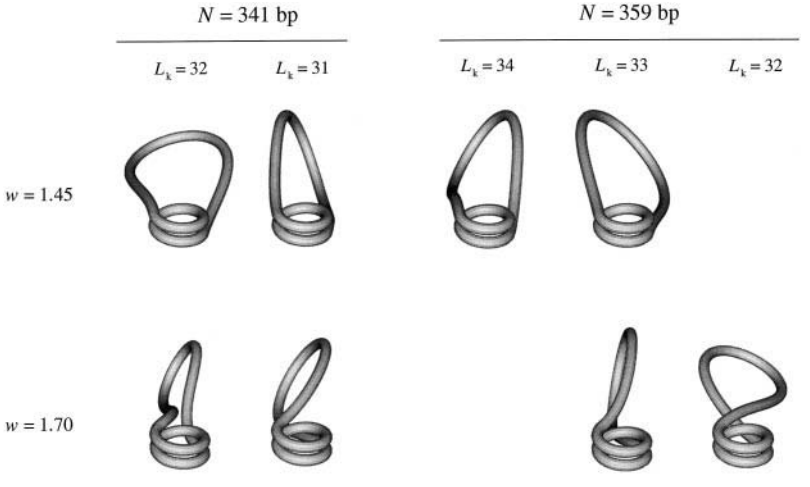

FIGURE 3 DNA minicircles in mononucleosomes depicted as tubes of diameter 20 Å. The line of view is here different from that of Fig. 2, but the values of h_0^b, w, L_k and the configurations are as in that figure.

TABLE 1 Calculated values of W_r, Ψ^*, and Δ for the configurations shown in Figs. 2 and 3

N	w	L_k	$L_k - N/h_0$	W_r	Ψ^* (kcal/mol)	Δ (nm)
341	1.45	31	−1.38	−1.19	6.76	9.4
341	1.45	32	−0.38	−0.83	6.53	9.4
341	1.70	31	−1.38	−1.56	6.54	6.5
341	1.70	32	−0.38	−0.45	10.90	2.5
359	1.45	33	−1.09	−1.08	4.93	9.4
359	1.45	34	−0.09	−0.61	8.12	9.4
359	1.70	32	−2.09	−1.89	8.40	3.8
359	1.70	33	−1.09	−1.46	6.84	6.8

topoisomer with $L_k = 33$ is expected to predominate. (The small value of Δ (3.8 nm) that we found for $N = 359$, $w = 1.45$, $L_k = 32$ indicates that even if electrostatic effects were taken into account, our conclusion to the effect that the topoisomer with $L_k = 33$ predominates would be expected to hold.) This conclusion about the predominance of $L_k = 33$ for both values of w holds not only for $h_0^b = 10.40$ bp/turn, but also for $h_0^b = 10.31$. In the case of $h_0^b = 10.53$ bp/turn, for $w = 1.45$ the conclusion holds again, but for $w = 1.70$ the energies for $L_k = 33$ and $L_k = 32$ differ by only 0.02 kcal/mol.

Zivanovic et al. (1988) also observed that for $N = 354$, relaxation of mononucleosomes yields topoisomers with $L_k = 32$ and 33. We find that these two values of L_k are in both $\mathcal{S}(354, 1.45, 10.40)$ and $\mathcal{S}(354, 1.70, 10.40)$, and they are the only values in those sets. When, in the following section, we discuss the implications of our theory for the interpretation of measurements of concentrations of topoisomers resulting from relaxation, we shall not go into detail for the case $N = 354$; for, as Ariel Prunell (Université Paris 7, personal communication, 1997) pointed out to us, the data of Zivanovic et al. (1988) for the distribution of L_k after relaxation with $N = 354$ cannot be taken to be reliable. As their figure 7 indicates, in that particular case the topoisomer distribution at the end of the relaxation experiment depended on the initial distribution and thus did not describe a state of equilibrium.

Fig. 4 contains graphs of W_r versus w at specified values of N, h_0^b, and values of L_k in $\mathcal{S}(N, w, h_0^b)$. The graphs shown were calculated using first the procedure described above to find $\mathcal{X}^*(\Lambda, w, h_0^b, L_k)$ and then the explicit results for Θ given in Eqs. B6–B12 to obtain W_r via Eq. B1. When N is fixed at 341 or 359 and h_0^b at 10.31, 10.40, or 10.53 bp/turn, there is but one value of L_k that is in the sets $\mathcal{S}(N, w, h_0^b)$ for all w in the range $1.2 \le w \le 1.9$. That value, $L_k^{\#}(N)$, corresponds to the topoisomer that Zivanovic et al. (1988) found to have the highest concentration upon completion of relaxation of mononucleosomes with the given N. There is a broad range of N for which $L_k^{\#}(N)$ is the (unique) value of L_k in $\mathcal{S}(N, w, h_0^b)$ for which the writhe of $\mathcal{C}$ is a continuous monotone decreasing function of wrap with W_r close to -1 for small w, close to -1.7 for large w. When $L_k = L_k^{\#}(N)$, a change in h_0^b from 10.31 to 10.53 at fixed w induces a change in W_r of at most 10%.

Now, let us recall that $\mathcal{S}(N, w, h_0^b)$ is the set of values of L_k for which there is no self-contact in the configuration that

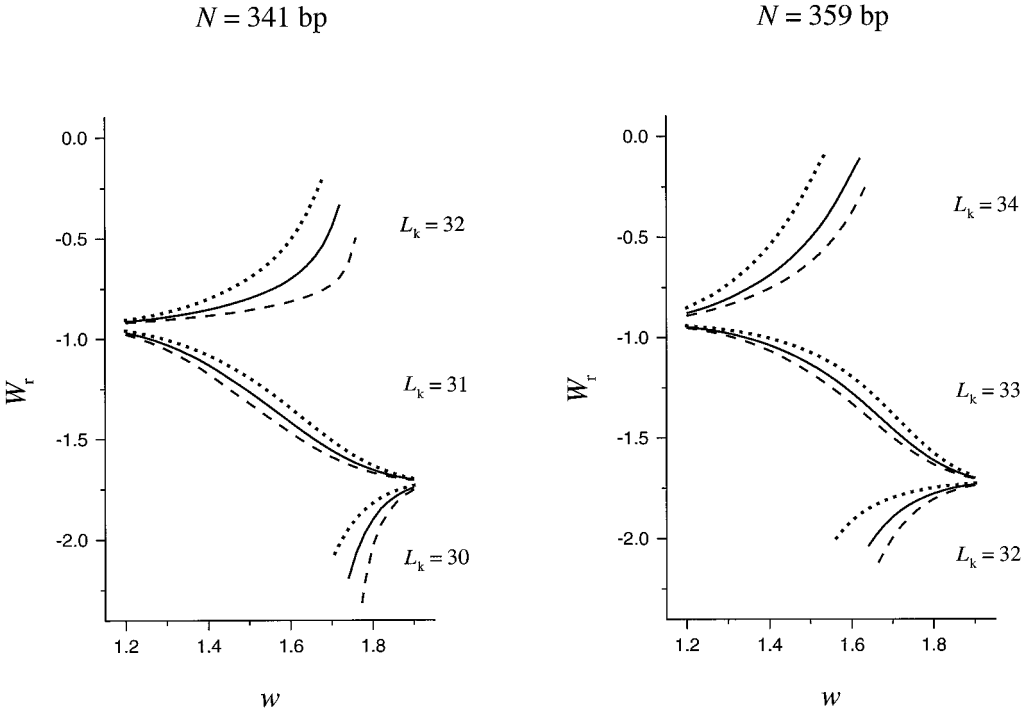

FIGURE 4 The writhe W_r for the configuration $\mathcal{X}^*$ versus the wrap w for two values of N and three values of h_0^b: 10.53 (••••), 10.40 (———), 10.31 (– – –) bp/turn. Each triple of solid, dotted, and dashed curves is for a topoisomer with the indicated value of L_k in $\mathcal{S}(N, w, h_0^b)$.

minimizes Ψ over the class of all configurations with the specified parameters (N, w, h_0^b, L_k). For Fig. 4, as for Figs. 2 and 3, the triplets (N, w, h_0^b) are such that $\mathcal{S}(N, w, h_0^b)$ contains two elements; one is $L_k = L_k^{\#}(N)$, and the other is $L_k^{\#}(N) + 1$ or $L_k^{\#}(N) - 1$. An exceptional case occurs when the quadruple (N, w, h_0^b, L_k) characterizes the special point σ_J on the curve ℓ^* discussed in the Remark of Appendix A. Such a special point occurs at critical value w_J of w at which one sees a jump of -2 in W_r (and hence in L_k) as one moves, in the direction of increasing w, along otherwise continuous curves in Fig. 4 on which W_r is monotone increasing in w. When we calculate W_r in a neighborhood of w_J, we ignore the constraint that $\mathcal{L}^*$ be free from self-contact, and we find that the geometry of the axial curve $\mathcal{C}^f$ for the minimum energy configuration is such that when $w = w_J$, the curve passes through itself, causing W_r to make a jump. Thus there is a sense in which, for each pair (N, h_0^b), the two separate continuous graphs on which W_r increases with w can be regarded as segments of one graph that contains a point of discontinuity and gives, as a function of w, the writhe of the minimum energy configuration for the element $L_k^{\diamond}$ of $\mathcal{S}(N, w, h_0^b)$ that is not equal to $L_k^{\#}(N)$; when N and h_0^b are fixed, $L_k^{\diamond}$ can vary with w, and the jump in W_r equals the corresponding jump in $L_k^{\diamond}$.

Having seen the strong dependence on L_k of graphs of W_r versus w, one may ask about the form of such graphs for cases in which the DNA in the extranucleosomal loop has been nicked, i.e., has had one of its duplex strands severed. For nicked DNA, W_r is independent of assumptions about h_0^b, and its calculation for minimum energy configurations is more easily performed. Tobias et al. (1994) and Coleman et al. (1995) have given a detailed account of the use of the method of exact solutions to obtain explicit expressions for equilibrium configurations of nicked DNA segments subject to boundary conditions of the type that occur here when N and w are specified (see Eqs. A20–A26). To obtain W_r from their formulae giving $\boldsymbol{r}(s)$, one can, for nicked DNA, use Eqs. B6–B12 with ω set equal to 0 in Eqs. B9–B11; for, in the theory of mechanical equilibrium, nicked DNA can be regarded as a special case of Kirchhoff's theory in which $\boldsymbol{M} \cdot \boldsymbol{t}$ has been set equal to 0, which is here equivalent to putting $\Delta\Omega^f = 0$. The resulting graphs of W_r versus w are given in Fig. 5. As that figure makes clear, for mononucleosomes containing nicked DNA with N in the range $330 \le N \le 370$, graphs of W_r versus w are nearly independent of N and, not surprisingly, have the monotonicity property of the corresponding graphs for cases in which the DNA is not nicked and has $L_k = L_k^{\#}(N)$.

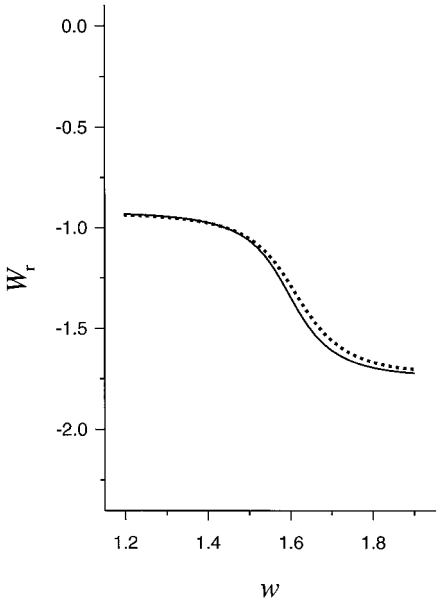

FIGURE 5 Writhe versus wrap for cases in which the extranucleosomal loop is nicked: $N = 330$ (•••) and $N = 370$ (———). The corresponding graphs for $N = 341$ and 359 lie between the two curves shown.

EQUILIBRIUM DISTRIBUTIONS OF TOPOISOMERS

For the values of w and N for which we report calculations, the size N^f of the free segment is between 178 and 274 bp. At the temperature at which measurements have been made of equilibrium distributions of topoisomers in mononucleosomes (Zivanovic et al., 1988), the persistence length a_p corresponding to the value of A employed for the calculations reported here is 141 bp, which implies that N^f is less than $2a_p$. With this observation in mind, we now make use of the assumption that the increment in the equilibrium free energy G of a mononucleosome due to a change in L_k at fixed w (and, of course, at fixed N and h_0^b) can be equated to the increment in Ψ^*_{N,w,h_0^b}, i.e., that

$$G(N, w, h_0^b, L_k^{(2)}) - G(N, w, h_0^b, L_k^{(1)}) = \Psi^*_{N,w,h_0^b}(L_k^{(2)}) - \Psi^*_{N,w,h_0^b}(L_k^{(1)}). \quad (18)$$

In the previous section we assembled the results that permit us to use this assumption to calculate equilibrium distributions of topoisomers.

If we suppose that all of the minicircles are in mononucleosomes with the same wrap w, then at equilibrium the fraction $P_{N,w,h_0^b}(L_k)$ of isomers with integral linking number L_k will be given by the equation

$$P_{N,w,h_0^b}(L_k) = Q^{-1}_{N,w,h_0^b} \exp\{-\Psi^*_{N,w,h_0^b}(L_k)/(RT)\}, \quad (19)$$

in which

$$Q_{N,w,h_0^b} = \sum_{L_k} \exp\{-\Psi^*_{N,w,h_0^b}(L_k)/(RT)\}. \quad (20)$$

Although in the most general case the sum in Eq. 20 would be taken over all integers, in accord with the discussion following Eq. 17, we here assume that only values of L_k in $\mathcal{S}(N, w, h_0^b)$ make a significant contribution to Q_{N,w,h_0^b}.

For the average value $\langle L_k \rangle_{N,w,h_0^b}$ of the integer L_k, we have

$$\langle L_k \rangle_{N,w,h_0^b} = \sum_{L_k} L_k P_{N,w,h_0^b}(L_k), \tag{21}$$

with the sum again over $\mathcal{S}(N, w, h_0^b)$. Implications of Eq. 19 for the relation between $\langle L_k \rangle_{N,w,h_0^b}$ and N are shown in Fig. 6 for wraps of 1.45 and 1.70 turns. The graphs given there for $h_0^b = 10.31$, 10.40, 10.53 show a repetitive structure of intervals on which $\langle L_k \rangle_{N,w,h_0^b}$ is approximately linear in N separated by intervals in which $\langle L_k \rangle_{N,w,h_0^b}$ is approximately constant at a value close to an integer (e.g., 30, 31, etc.).

The dependence of $P_{N,w,h_0^b}(L_k)$, and hence of $\langle L_k \rangle_{N,w,h_0^b}$, on h_0^b is determined by the following useful fact: when Eq. 15 is solved for $\Delta\Omega^f$ with N and w fixed, $\Delta\Omega^f$ is a function of $L_k - (N_0^b/h_0^b)$ alone, and hence Eqs. 16 and 17 tell us that for each pair (N, w) there is a function $\hat{\Psi}_{N,w}$ that (1) is independent of h_0^b, (2) is defined for noninteger arguments, and (3) for each integer L_k in $\mathcal{S}(N, w, h_0^b)$ obeys the relation

$$\Psi^*_{N,w,h_0^b}(L_k) = \hat{\Psi}_{N,w}(L_k - (N_0^b/h_0^b)). \tag{22}$$

As the mathematical treatment that in the previous section enabled us to characterize minimum energy configurations remains valid (under an appropriate modification of the definition of the set $\mathcal{S}(N, w, h_0^b)$) when L_k is taken to be a nonintegral number, our procedure for calculating Ψ^*_{N,w,h_0^b} can be applied to determine the function $\hat{\Psi}_{N,w}$ on an interval.

For each triple (N, w, h_0^b) the function P_{N,w,h_0^b}, giving the fraction $P_{N,w,h_0^b}(L_k)$ of topoisomers with integral linking number, is determined by the following probability density function ρ_{N,w,h_0^b} for a continuous distribution of linking number:

$$\rho_{N,w,h_0^b}(L_k) = q_{N,w}^{-1} \exp\{-\hat{\Psi}_{N,w}(L_k - (N_0^b/h_0^b))/(RT)\}. \tag{23}$$

Here the normalizing coefficient,

$$q_{N,w} = \int \exp\{-\hat{\Psi}_{N,w}(L_k - (N_0^b/h_0^b))/(RT)\} dL_k, \tag{24}$$

is independent of h_0^b. The integral in Eq. 24 is taken over all L_k in the interval $I(N, w, h_0^b)$ defined in the Remark of Appendix A. When L_k is an integer,

$$P_{N,w,h_0^b}(L_k) = (q_{N,w}/Q_{N,w,h_0^b}) \rho_{N,w,h_0^b}(L_k). \tag{25}$$

In cases in which all of the bound (i.e., nucleosomal) DNA has twist density $\Omega_0^b = 2\pi/(0.34 h_0^b)$, and hence no bound DNA is torsionally equilibrated with $\mathcal{R}^f$, N_0^b in Eqs. 22–24 is to be replaced by N^b.

The continuous distribution ρ_{N,w,h_0^b} is expected to be appropriate to mononucleosomes for which the extranucleosomal loop $\mathcal{R}^f$ has been nicked. For nicked plasmids one can use Eq. 2 as a definition of L_k, and ρ_{N,w,h_0^b} is then the probability density function for thermal fluctuations in L_k. (Once again, we assume that N^f is such that the free energy change associated with a change in L_k at fixed w can be identified with the difference in Ψ-values for the corresponding minimum energy configurations; this assumption is crucial if a distribution computed using Eq. 24 is to be identified with one due to thermal fluctuations.)

Despite the chiral bias that one might expect to result from the helicity of $\mathcal{R}^b$, when we put into Eq. 23 precisely calculated results for $\hat{\Psi}_{N,w}$, we find that ρ_{N,w,h_0^b} shows no apparent skewness and departs only slightly from a Gaussian probability density function ρ^G of the type employed in analyses of relaxation experiments on protein-free circular DNA (cf. Shore and Baldwin, 1983; Horowitz and Wang, 1984):

$$\rho^G = \sqrt{K/\pi} \exp\{-K(L_k - \bar{L}_k)^2\}. \tag{26}$$

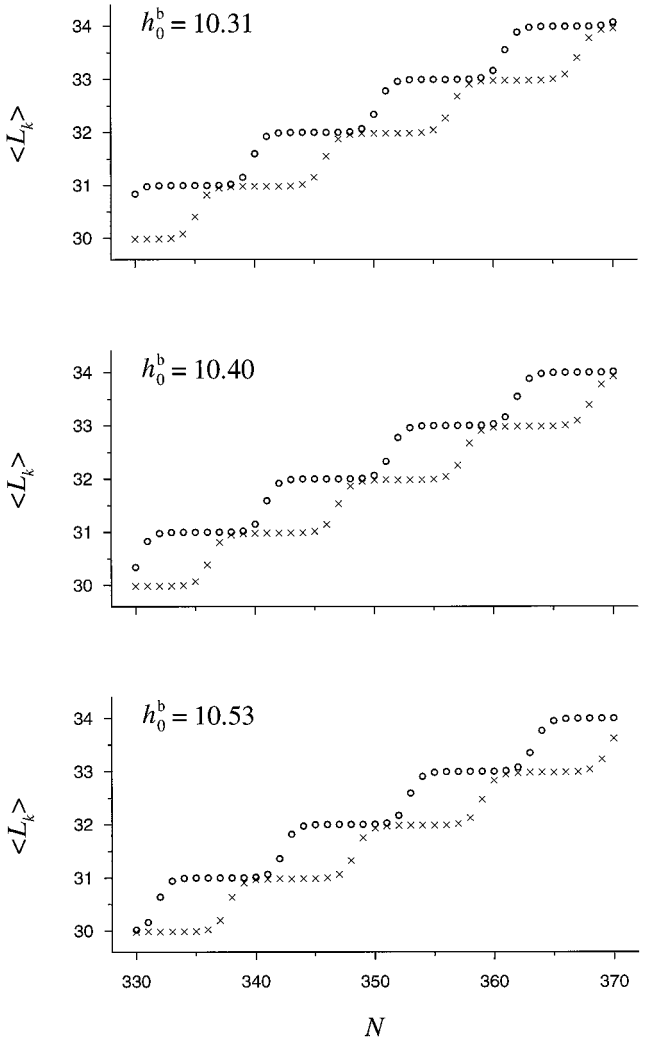

FIGURE 6 Results of a calculation of the dependence on N of the average, $\langle L_k \rangle$, of the integral values of L_k present in an equilibrium mixture of topoisomers obtained by relaxation of DNA minicircles in mononucleosomes. This calculation is based on the supposition that the wrap w is fixed with $w = 1.45$ (○) or $w = 1.70$ (×).

In Eq. 26, $\bar{L}_k$ is the value of L_k that minimizes $\hat{\Psi}_{N,w}(L_k - (N_0^b/h_0^b))$ at fixed (N, w, h_0^b), and K is proportional to the corresponding second derivative of $\hat{\Psi}_{N,w}$:

$$\hat{\Psi}_{N,w}(\bar{L}_k - (N_0^b/h_0^b)) = \min_{L_k} \hat{\Psi}_{N,w}(L_k - (N_0^b/h_0^b)), \quad (27a)$$

$$K = K(N, w) = \frac{1}{2RT}\frac{\partial^2}{\partial L_k^2}\hat{\Psi}_{N,w}(L_k - (N_0^b/h_0^b))\big|_{L_k=\bar{L}_k}; \quad (27b)$$

K is measured in units of RT. As $\bar{L}_k$, the value of L_k at which the (continuous) density function ρ_{N,w,h_0^b} has its maximum value, turns out to be very close to the average value of the distribution with density ρ_{N,w,h_0^b}, we shall identify $\bar{L}_k$ with that average; $\bar{L}_k$ should not, however, be confused with $\langle L_k \rangle$, the average of an appropriate sampling of integral values of L_k. (Of course, $\bar{L}_k$ is precisely the average value of the (continuous) Gaussian distribution approximating that of ρ_{N,w,h_0^b}.) Graphs of ρ_{N,w,h_0^b} and its approximation ρ^G are shown in Fig. 7 for $N = 341$ and 359 with $w = 1.45$ and 1.70. Table 2 contains the corresponding computed values of $\bar{L}_k$ and K.

Fig. 8 shows the dependence on N of calculated values of N^fK, $\bar{L}_k$, and $\bar{L}_k - (N/h_0)$ (for $h_0^b = 10.40$ and fixed w). We note that N^fK, which is here the analog of the quantity NK occurring in discussions of the free energy of supercoiling of protein-free plasmids, is approximately linear in N with a slope that depends on w and is positive for $w = 1.45$ and negative for $w = 1.70$. In particular, as N increases from 330 to 370, N^fK decreases by 6% when $w = 1.45$ and increases by 2% when $w = 1.70$. As expected, the variation of $\bar{L}_k$ with N is very close to linear, and most of that variation is accounted for by N/h_0. The results shown in Fig. 7 can be summarized as follows: To within the precision of our calculations,

$$N^fK(N, 1.45) = 2731 - 4(N - 330), \quad (28a)$$

$$\bar{L}_k(N, 1.45, 10.40) = N/h_0 - 0.87; \quad (28b)$$

$$N^fK(N, 1.70) = 2345 + (N - 330), \quad (29a)$$

$$\bar{L}_k(N, 1.70, 10.40) = N/h_0 - 1.42 - 1.2 \times 10^{-3}(N - 330). \quad (29b)$$

As our notation indicates, K is independent of h_0^b. It is not difficult to show that Eq. 27a implies that, for any two values $h_0^b(1)$, $h_0^b(2)$ of h_0^b,

$$\bar{L}_k(N, w, h_0^b(2)) = \bar{L}_k(N, w, h_0^b(1)) - \frac{N_0^b}{h_0^b(1)} + \frac{N_0^b}{h_0^b(2)}. \quad (30)$$

Here, once again, when all of the nucleosomal DNA has twist density $2\pi/(0.34h_0^b)$, N_0^b is to be replaced by N^b.

The dependence of $\rho_{N,w,h_0^b}(L_k)$ on h_0^b (expressed in Eq. 23) and its consequences, namely Eq. 30 and the conclusion that K is independent of h_0^b, all follow from Eqs. 15 and 16. One may ask if the dependence of $\rho_{N,w,h_0^b}(L_k)$ and related quantities on N can be rendered explicit. The answer is yes if one is content with approximations; for a careful examination of the calculation of $\tilde{W}_r(\Delta\Omega^f; \Lambda, w)$ and $\tilde{\Psi}(\Delta\Omega^f; \Lambda, w)$ tells one that there are functions Φ_w such that approximation formu-

TABLE 2 Calculated values of parameters of the Gaussian probability density functions, shown as dashed lines in Fig. 7

N	w	$\bar{L}_k$	$\bar{L}_k - N/h_0$	K (RT)	$N^f K$ (RT)
341	1.45	31.52	−0.87	7.35	2687
341	1.70	30.94	−1.44	7.07	2357
359	1.45	33.22	−0.87	6.62	2617
359	1.70	32.63	−1.46	6.55	2375

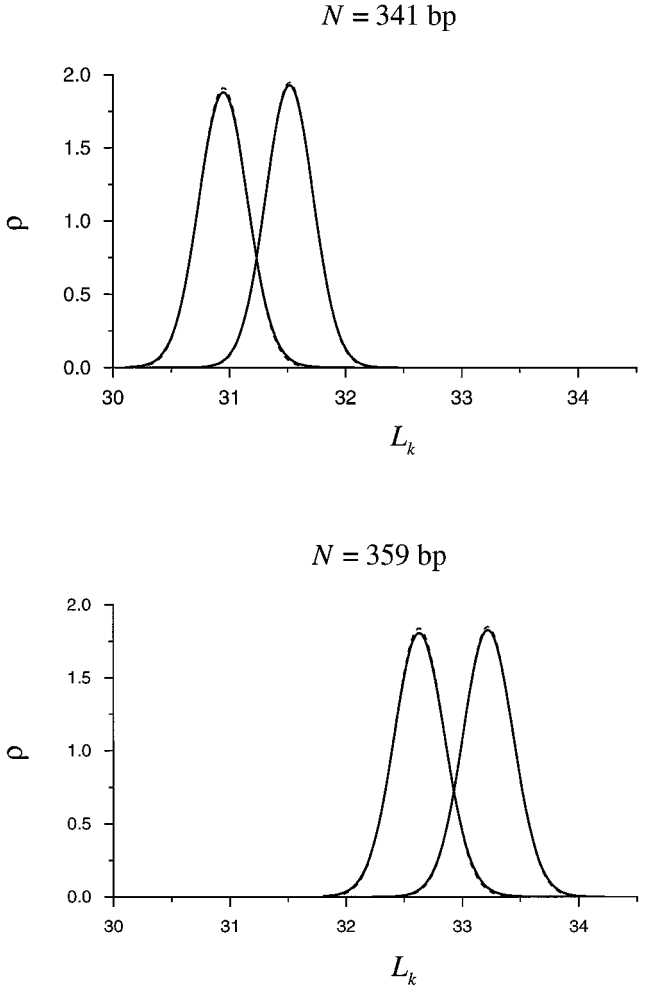

FIGURE 7 Probability density functions $\rho = \rho_{N,w,h_0^b}$ for hypothetical continuous distributions of linking number at fixed wrap for DNA minicircles in mononucleosomes (see Eqs. 23 and 24). For each N, the wrap w is 1.70 for the bell-shaped curve on the left and 1.45 for the one on the right. The dashed curves are graphs of the Gaussian probability density functions ρ^G that for given (N, w, h_0^b) approximate ρ_{N,w,h_0^b} are in accord with Eqs. 26 and 27. The density functions shown were calculated supposing that $h_0^b = 10.40$ bp/turn; a change in h_0^b results in a translation of each curve along the L_k axis, in accord with Eq. 23.

lae of the type

$$N^{f}\hat{\Psi}_{N,w}(L_k - (N_0^b/h_0^b)) \cong \Phi_w(L_k - (N_0^b/h_0^b) - (N/h_0)) \tag{31}$$

are useful for sufficiently small ranges of N, the length of which depends on the value of w. This result implies, in turn, the existence of functions $\check{\rho}_w$ such that

$$\rho_{N,w,h_0^b}(L_k) \cong \check{\rho}_w(L_k - (N_0^b/h_0^b) - (N/h_0)). \tag{32}$$

If this approximate expression for ρ_{N,w,h_0^b} were taken to be exact, one would conclude that there is a function g_w such that Eq. 21 can be written as $\langle L_k\rangle_{N,w,h_0^b} = g_w((N_0^b/h_0^b) + (N/h_0))$, and that N^fK is independent of N and that $\bar{L}_k$ is given by a relation of the form

$$\bar{L}_k = N/h_0 - \check{L}(w, h_0^b), \tag{33}$$

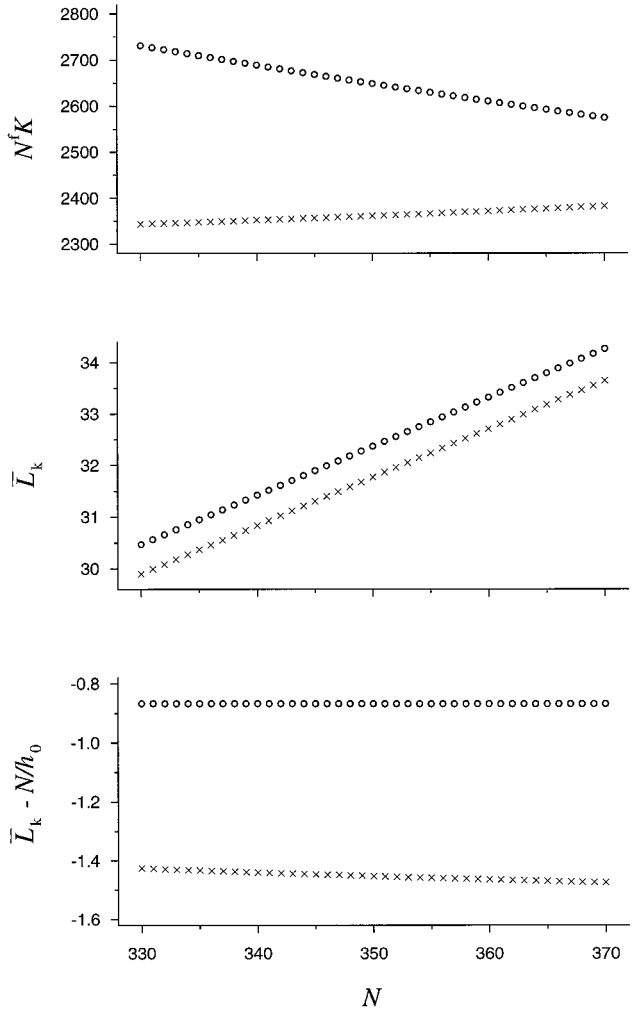

FIGURE 8 Results of calculations of the dependence on N of the parameters K and $\bar{L}_k$ of Eq. 27 for $w = 1.45$ (○) and $w = 1.70$ (×). In each case, $h_0^b = 10.40$ bp/turn.

with $\check{L}(w, h_0^b)$ independent of N. (By coincidence, as we see in Eq. 28b, Eq. 33 is very close to an exact relation for $330 \le N \le 370$ when $w = 1.45$.)

Electron micrographs published by Zivanovic et al. (1988) for $N = 359$ indicate that when a minicircle of the size we are considering here is in a mononucleosome, w can have various values. We are now in a position to derive implications of the present theory about the effect of fluctuations in w on equilibrium distributions of L_k. Although, for simplicity of presentation, we shall confine our discussion to a case in which w fluctuates between two values, $w^{(1)}$, $w^{(2)}$, with $w^{(2)} > w^{(1)}$, the generalization of our principal results to a multistate model with an arbitrary number of possible values for w will be evident. In the discussion that follows, we generally do not render explicit the parameters (i.e., N and h_0^b) that are assumed to be the same for all the mononucleosomes in an equilibrium mixture.

For a mononucleosome with a given value of L_k, a change in w from $w^{(1)}$ to $w^{(2)}$ induces a increment $\Delta G(w^{(1)}, w^{(2)}, L_k)$ in the free energy G of Eq. 18. Let Γ be that part of $\Delta G(w^{(1)}, w^{(2)}, L_k)$ that is not accounted for by the change in the elastic energy Ψ^*:

$$\Gamma = G(w^{(2)}, L_k) - G(w^{(1)}, L_k) - (\Psi^*_{w^{(2)}}(L_k) - \Psi^*_{w^{(1)}}(L_k)). \tag{34}$$

As Eq. 18 implies that for each pair (w, L_k)

$$G(w, L_k) = G^0(w) + \Psi^*_w(L_k), \tag{35}$$

Γ is independent of L_k, i.e.,

$$\Gamma = \Gamma(w^{(1)}, w^{(2)}) = G^0(w^{(2)}) - G^0(w^{(1)}). \tag{36}$$

Let $P(L_k)$ (i.e., $P_{N,h_0^b}(L_k)$) be the fraction of the mononucleosomes that have integral linking number L_k in a mixture of topoisomers for which the wrap is fluctuating between $w^{(1)}$ and $w^{(2)}$. When equilibrium is established with respect to both L_k and w,

$$P(L_k) = Q^{-1}\left(\exp\left\{\frac{-\Psi^*_{w^{(1)}}(L_k)}{RT}\right\} + \exp\left\{\frac{-\Psi^*_{w^{(2)}}(L_k) - \Gamma(w^{(1)}, w^{(2)})}{RT}\right\}\right), \tag{37}$$

$$Q = \sum_{L_k}\left(\exp\left\{\frac{-\Psi^*_{w^{(1)}}(L_k)}{RT}\right\} + \exp\left\{\frac{-\Psi^*_{w^{(2)}}(L_k) - \Gamma(w^{(1)}, w^{(2)})}{RT}\right\}\right); \tag{38}$$

here the sum is to be taken over those values of L_k that are in either one or both of the two sets $\mathcal{S}(w^{(1)})$, $\mathcal{S}(w^{(2)})$, with $\Psi^*_{w^{(i)}}(L_k)$ set equal to $+\infty$ for any L_k not in the corresponding $\mathcal{S}(w^{(i)})$.

The probability density function ρ for a continuous distribution that, by a formula analogous to Eq. 25, determines

$P(L_k)$ for integer L_k is

$$\rho(L_k) = q^{-1}\left(\exp\left\{\frac{-\hat{\Psi}_{w^{(1)}}(L_k - (N_0^b/h_0^b))}{RT}\right\} + \exp\left\{\frac{-\hat{\Psi}_{w^{(2)}}(L_k - (N_0^b/h_0^b)) - \Gamma(w^{(1)}, w^{(2)})}{RT}\right\}\right), \tag{39}$$

$$q = \int\left(\exp\left\{\frac{-\hat{\Psi}_{w^{(1)}}(L_k - (N_0^b/h_0^b))}{RT}\right\} + \exp\left\{\frac{-\hat{\Psi}_{w^{(2)}}(L_k - (N_0^b/h_0^b)) - \Gamma(w^{(1)}, w^{(2)})}{RT}\right\}\right)dL_k; \tag{40}$$

the integral in Eq. 40 is taken over the union of the intervals $I(w^{(1)})$ and $I(w^{(2)})$, with $\hat{\Psi}_{w^{(i)}}(L_k - (N_0^b/h_0^b))$ set equal to $+\infty$ for L_k not in $I(w^{(i)})$.

It follows from Eq. 37 that when one knows the ratio, $P(L_k^{(A)})/P(L_k^{(B)})$, of the equilibrium concentrations of any two topoisomers with linking numbers in the union of $\mathcal{S}(w^{(1)})$ and $\mathcal{S}(w^{(2)})$, one can calculate $\Gamma(w^{(1)}, w^{(2)})$ as follows:

$$\Gamma(w^{(1)}, w^{(2)}) = -RT\ln\left(\left[\exp\left\{\frac{-\Psi^*_{w^{(1)}}(L_k^{(A)})}{RT}\right\} - \frac{P(L_k^{(A)})}{P(L_k^{(B)})}\exp\left\{\frac{-\Psi^*_{w^{(1)}}(L_k^{(B)})}{RT}\right\}\right]\Big/\left[\frac{P(L_k^{(A)})}{P(L_k^{(B)})}\exp\left\{\frac{-\Psi^*_{w^{(2)}}(L_k^{(B)})}{RT}\right\} - \exp\left\{\frac{(-\Psi^*_{w^{(2)}}(L_k^{(A)})}{RT}\right\}\right]\right) \tag{41}$$

Zivanovic et al. (1988) reported that their measurements of ratios $P(L_k^{(A)})/P(L_k^{(B)})$ of equilibrium concentrations for the relaxation with topoisomerase I of minicircles in mononucleosomes gave the following results: for $N = 341$, $P(32)/P(31) = 0.25$; for $N = 359$, $P(33) \cong 1$. Taking $w^{(1)}$ to be 1.45 and $w^{(2)}$ to be 1.70, assuming that h_0^b is 10.40, and using the calculated values of Ψ^*_{N,w,h_0^b} given in Table 1, we find that a value of 0.75 kcal/mol for $-\Gamma(1.45, 1.70)$ is in accord with their observations, for it yields 0.25 for $P(32)/P(31)$ when $N = 341$. (It yields 0.99 for $P(33)$ when $N = 359$, but at that value of N a broad range of values of Γ would yield a value close to 1 for $P(33)$.) This estimate of 0.75 kcal/mol for the two segments $\mathcal{R}_-^b$, $\mathcal{R}_+^b$, i.e., of 0.04 kcal/mol of base pairs, is smaller than the value 0.1–0.15 kcal/mol bp that is consistent with results that Polach and Widom (1995, 1996) obtained using restriction endonuclease probes to measure the accessibility of sites within a nucleosome core particle as a function of distance from the ends (see the review of Felsenfeld, 1996).

The severity of the difficulties accompanying the use of the available measurements of topoisomer distributions to obtain binding energies was discussed at the end of the Introduction. Despite these difficulties, to have examples to examine, we offer in Fig. 9 graphs of ρ and P calculated

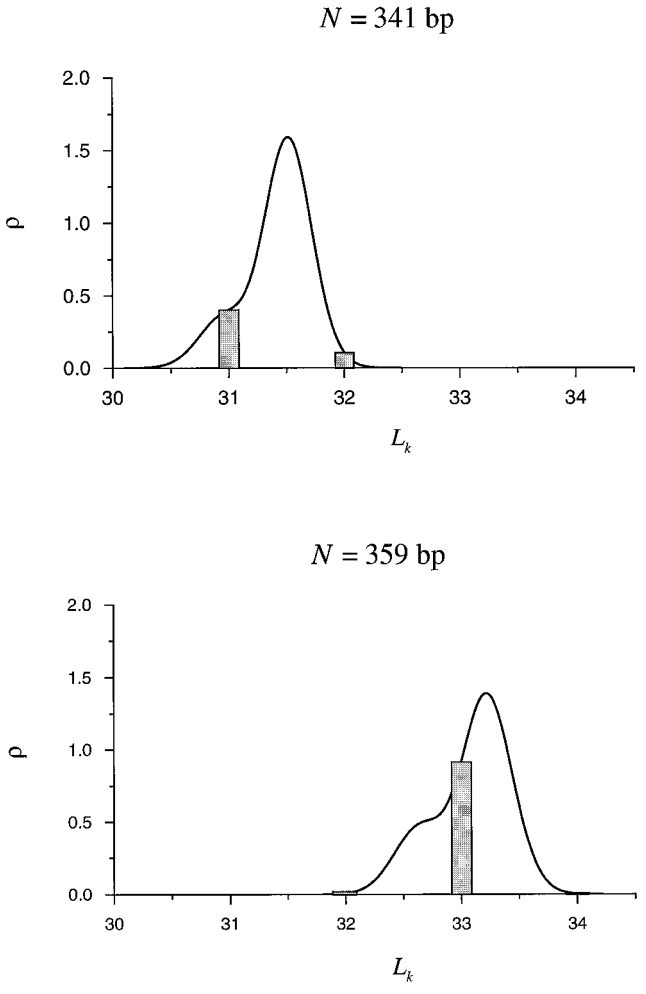

FIGURE 9 Probability density functions ρ for hypothetical continuous distributions of linking number for DNA minicircles in mononucleosomes with two possible states of wrap, $w^{(1)} = 1.45$ and $w^{(2)} = 1.70$ (see Eqs. 39 and 40). The heights of the shaded columns are proportional to the probability $P(L_k)$ that a topoisomer has linking number L_k in equilibrium (Eqs. 37 and 38). For these calculations it was assumed that $h_0^b = 10.40$ and $\Gamma(1.45, 1.70) = -0.75$.

with $\Gamma(1.45, 1.70) = -0.75$. As those graphs show, multistate models for equilibrium distributions of linking number can yield probability density functions that are not Gaussian, but instead are far from symmetric and, in extreme cases, bimodal, and thus very different from what one would find if all of the mononucleosomes had the same value of w during relaxation.

If we add to the rough approximations we have made in discussing the binding energy term Γ the further assumption that the function G^0 in Eq. 35 is linear in w, i.e., that to within an added constant (which we can identify with $G^0(w^{(1)})$),

$$G^0(w) = \frac{\Gamma(w^{(1)}, w^{(2)})}{w^{(2)} - w^{(1)}}(w - w^{(1)}), \tag{42}$$

then we can employ our method of calculating $\Psi^*_{N,w,h_0^b}(L_k)$ to make graphs of $G(w, L_k)$ as a function of w for fixed L_k.

Such graphs are shown in Fig. 10 for the values of L_k for which graphs of W_r versus w are seen in Fig. 4.

For the results shown in Fig. 10 we have put $\Gamma(1.45, 1.70) = -0.75$ and $h_0^b = 10.40$. The gaps seen there in otherwise smooth curves span neighborhoods of the values w_J of w at which $\mathscr{C}^f$ would pass through itself if the constraint that $\mathscr{R}^f$ is to be free from self-contact were ignored. It turns out that each local minimum in the plot of $G(w, L_k)$ versus w occurs near one of the two values of w, i.e., 1.45 and 1.70, employed for the two-state model.

APPENDIX A: DETERMINATION OF EQUILIBRIUM CONFIGURATIONS

By making use of Eq. 6, which asserts that $\boldsymbol{F}$ is constant in s, one may integrate Eq. 7 to obtain the relation $\boldsymbol{M} = \boldsymbol{F} \times \boldsymbol{r} + \boldsymbol{M^0}$, in which the vector $\boldsymbol{M^0}$ is a constant that depends on the choice of the origin **O** for $\boldsymbol{r}$. We choose **O** so that $\boldsymbol{M^0}$ is parallel to $\boldsymbol{F}$. For the explicit representation of equilibrium configurations of DNA segments subject to geometric end conditions (see, e.g., Tobias et al., 1994; Coleman et al., 1995), it is convenient to employ a system of cylindrical coordinates (r, ϕ, z) that was introduced by Landau and Lifshitz (1986). The z axis for that system is parallel to $\boldsymbol{F}$ and contains the point **O**.

The number ω, defined by

$$\omega = \frac{C}{A}\sqrt{\frac{2A}{F}}\,\Delta\Omega^f, \tag{A1}$$

where $F = |\boldsymbol{F}|$, is independent of s and serves as a dimensionless measure of the excess twist density.

In this appendix we shall use $\sqrt{2A/F}$ as the unit of length. When this is done, the relation $\boldsymbol{M} = \boldsymbol{F} \times \boldsymbol{r} + \boldsymbol{M^0}$ and Eq. 8 yield

$$\boldsymbol{r}' \times \boldsymbol{r}'' + \omega \boldsymbol{r}' = 2[\boldsymbol{k} \times \boldsymbol{r} + \lambda \boldsymbol{k}], \tag{A2}$$

where $\boldsymbol{k}$ is a unit vector in the direction of increasing z, and λ is a constant. For each choice of λ and ω, Eq. A2 is a system of three differential equations that one can solve to obtain the vector-valued function, $\boldsymbol{r} = \boldsymbol{r}(s)$ that describes the curve $\mathscr{C}^f$.

In the units we are using, the quantities s, r, z, ω, λ, $\boldsymbol{M}$, as well as the curvature κ and geometric torsion τ of $\mathscr{C}^f$, are dimensionless. For the dimensionless length of $\mathscr{C}^f$ we write Σ:

$$\Sigma = \Lambda^f \sqrt{F/2A}. \tag{A3}$$

We take the midpoint of $\mathscr{C}^f$ to be the point where $s = 0$, and hence at the end points we have

$$s_A = -\Sigma/2, \qquad s_B = \Sigma/2. \tag{A4}$$

Let (x, y, z) be Cartesian coordinates, with the z axis as above and the x axis containing the midpoint of $\mathscr{C}^f$. The relations

$$x = r\cos\phi, \qquad y = r\sin\phi \tag{A5}$$

complete the definition of the coordinates (r, ϕ, z). In terms of these coordinates, the condition of inextensibility, $(x')^2 + (y')^2 + (z')^2 = 1$, becomes

$$(r')^2 = u(\phi')^2 + (z')^2, \tag{A6}$$

where $u = r^2$. We note in passing (cf. Tobias et al., 1994) that Eq. A2 permits us to express κ a function of λ, r and ω,

$$\kappa^2 = 4(r^2 + \lambda^2) - \omega^2, \tag{A7}$$

and τ as a function of κ, λ, ω, and another constant of integration a:

$$\tau = \frac{1}{2}\omega - \left[4\lambda + \frac{1}{2}\omega^3 - 2\omega(\lambda^2 + a)\right]\kappa^{-2}. \tag{A8}$$

Equation A8, which will be employed in Appendix B, is the form here taken by a general "torsion-curvature" relation, $\kappa^2(s)[\tau(s) - \frac{1}{2}\omega] = f(\omega)$, that holds for both equilibrium and traveling wave solutions in Kirchhoff's theory of rods (cf. Coleman et al., 1993).

When Eq. A2 is expressed in the cylindrical coordinates (r, ϕ, z) and combined with Eq. A6, the general solution of the resulting system is

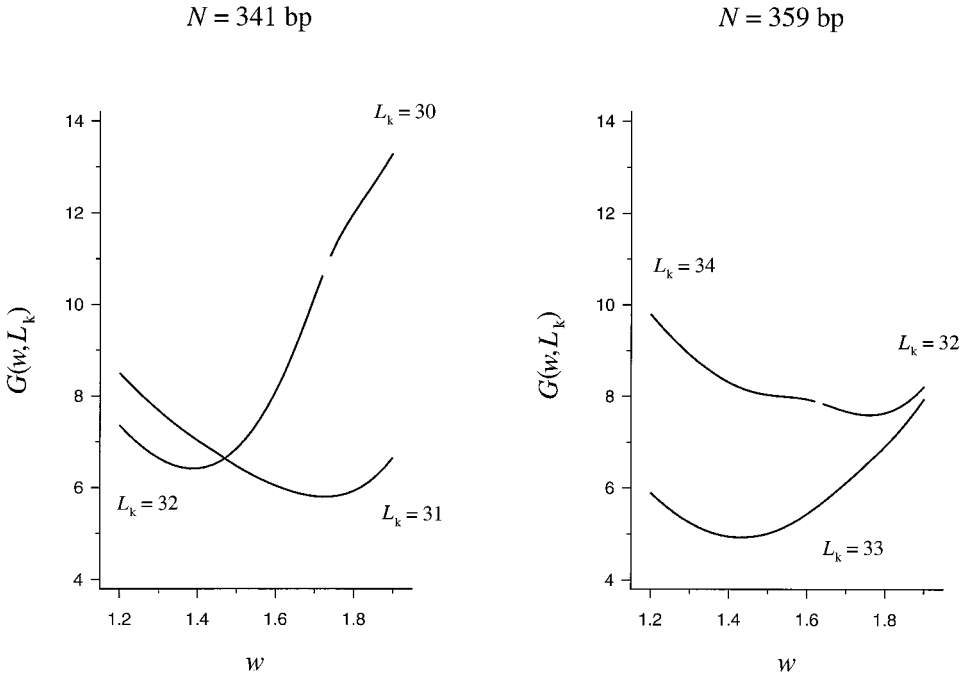

FIGURE 10 The sum $G(w, L_k)$ of $G^0(w)$ and the elastic energy $\Psi_w^*(L_k)$ (in kcal/mol of nucleosomes) as a function of w at fixed L_k. These graphs were constructed assuming that $h_0^b = 10.40$, and using Eq. 42 with $\Gamma(1.45, 1.70) = -0.75$.

(Tobias et al., 1994; Coleman et al., 1995):

$$r^2 = u_3 - (u_3 - u_2)\sin^2\psi, \tag{A9}$$

$$\phi = \lambda s + \frac{[(\omega/2) - \lambda a]\Pi(n;\psi|m)}{u_3\sqrt{u_3 - u_1}}, \tag{A10}$$

$$z = (a - u_1)s - \sqrt{u_3 - u_1}\,\mathrm{E}(\psi|m), \tag{A11}$$

where a is as in Eq. A8,

$$\sin\psi = \mathrm{sn}(s\sqrt{u_3 - u_1}), \qquad \text{i.e., } s = \mp\frac{\mathrm{F}(\psi|m)}{\sqrt{u_3 - u_1}}, \tag{A12}$$

$$m = (u_3 - u_2)/(u_3 - u_1), \qquad n = (u_3 - u_2)/u_3, \tag{A13}$$

and the u_i, with $u_1 \le 0 \le u_2 \le u_3$, are roots of the cubic polynomial

$$P_3(u) = -\left[u^3 + (\lambda^2 - 2a)u^2 + (a^2 - 2a\lambda^2 + \omega\lambda - 1)u + \left(\frac{\omega}{2} - a\lambda\right)^2\right] = (u - u_1)(u - u_2)(u_3 - u). \tag{A14}$$

In Eqs. A10–A12, sn is a Jacobi elliptic function with parameter m, and F, E, Π are the elliptic integrals,

$$\mathrm{F}(\psi|m) = \int_0^{\psi}\frac{\mathrm{d}\zeta}{\sqrt{1 - m\sin^2\zeta}}, \tag{A15}$$

$$\mathrm{E}(\psi|m) = \int_0^{\psi}(1 - m\sin^2\zeta)^{1/2}\mathrm{d}\zeta, \tag{A16}$$

$$\Pi(n;\psi|m) = \int_0^{\psi}\frac{\mathrm{d}\zeta}{(1 - n\sin^2\zeta)\sqrt{1 - m\sin^2\zeta}}. \tag{A17}$$

It follows from Eqs. A9–A14 that because the three numbers a, λ, ω determine the numbers u_1, u_2, u_3, the four numbers a, λ, Σ, ω determine the curve $\mathscr{C}^{\mathrm{f}}$ to within the scale factor $\sqrt{2A/F}$. In other words, for each choice of ω there is a three-parameter family of solutions. The three parameters to be fixed are the integration constants a and λ, and the dimensionless length Σ.

The elastic energy Ψ^{f} of the segment $\mathscr{R}^{\mathrm{f}}$ is defined in Eq. 11. A recent result (Coleman et al., 1995) gives us the following useful formula for Ψ^{f} at equilibrium:

$$\Psi^{\mathrm{f}} = \frac{2A\,\Sigma^2}{\Lambda^{\mathrm{f}}}\left[a + \lambda^2 - \zeta + \frac{1}{4}\left(\frac{A}{C} - 1\right)\omega^2\right]; \tag{A18}$$

here,

$$\zeta = [z(\Sigma/2) - z(-\Sigma/2)]/\Sigma. \tag{A19}$$

The procedure we employ for finding the triplet (a, λ, Σ) when there are given ω and geometric boundary data, $\boldsymbol{r}(s_{\mathrm{A}}) - \boldsymbol{r}(s_{\mathrm{B}})$, $\boldsymbol{t}(s_{\mathrm{A}})$, $\boldsymbol{t}(s_{\mathrm{B}})$, makes use of the fact that when $\boldsymbol{r}(s_{\mathrm{A}}) - \boldsymbol{r}(s_{\mathrm{B}})$ and Λ^{f} are known in conventional units, one knows the ratio

$$\eta = |\boldsymbol{r}(-\Sigma/2) - \boldsymbol{r}(\Sigma/2)|/\Sigma, \tag{A20}$$

and the vector

$$\boldsymbol{\nu} = \frac{\boldsymbol{r}(-\Sigma/2) - \boldsymbol{r}(\Sigma/2)}{|\boldsymbol{r}(-\Sigma/2) - \boldsymbol{r}(\Sigma/2)|}. \tag{A21}$$

In the present case the boundary data are symmetric in the sense that $\mathbf{t}(-\Sigma/2)\cdot\boldsymbol{\nu} = \mathbf{t}(\Sigma/2)\cdot\boldsymbol{\nu}$, and it therefore is convenient to describe the relative orientation of vectors $\boldsymbol{t}(-\Sigma/2)$, $\boldsymbol{t}(\Sigma/2)$, and $\boldsymbol{\nu}$ by giving the angles α and β for which

$$\cos\alpha = \boldsymbol{t}(\Sigma/2)\cdot\boldsymbol{\nu}, \tag{A22}$$

$$\sin\beta = \frac{\boldsymbol{t}(\Sigma/2)\cdot[\boldsymbol{\nu}\times\boldsymbol{t}(-\Sigma/2)]}{|\boldsymbol{t}(-\Sigma/2) - \boldsymbol{t}(\Sigma/2)|}. \tag{A23}$$

Our assumption that $\boldsymbol{r}(s)$ and $\boldsymbol{t}(s)$ are continuous for all s implies that the values of $\boldsymbol{r}(-\Sigma/2)$, $\boldsymbol{r}(\Sigma/2)$, $\boldsymbol{t}(-\Sigma/2)$, and $\boldsymbol{t}(\Sigma/2)$ entering Eqs. A20–A23 pertain to the end points of the helical curve $\mathscr{C}^{\mathrm{b}}$, and thus we can express (η, α, β) in terms of the pitch p, diameter d, and wrap w of $\mathscr{C}^{\mathrm{b}}$, and the length Λ of $\mathscr{C}$. We find that

$$\eta = \frac{\sqrt{d^2\sin^2(w\pi) + p^2w^2}}{\Lambda - w\sqrt{\pi^2d^2 + p^2}}, \tag{A24}$$

$$\cos\alpha = \frac{(1/2)\pi d^2\sin(2w\pi) + p^2w}{\sqrt{(d^2\sin^2(w\pi) + p^2w^2)(\pi^2d^2 + p^2)}}, \tag{A25}$$

$$\sin\beta = \frac{pd[\sin(w\pi) - w\pi\cos(w\pi)]}{\sqrt{(d^2\sin^2(w\pi) + p^2w^2)(\pi^2d^2 + p^2)}}. \tag{A26}$$

As we have observed, when ω is specified, Eqs. A9–A14 permit one to find the curve $\mathscr{C}^{\mathrm{f}}$ to within a scale factor and to determine the mapping $(a, \lambda, \Sigma) \mapsto (\eta, \alpha, \beta)$; one can automate the procedure of inverting this mapping to obtain (a, λ, Σ) from boundary data. Once Σ is determined, knowledge of the length Λ^{f} ($= \Lambda - 27.2w$) of $\mathscr{C}^{\mathrm{f}}$ in nm yields the scale factor $\sqrt{2A/F} = \Sigma/\Lambda^{\mathrm{f}}$ and thus the coefficient of proportionality between $\Delta\Omega^{\mathrm{f}}$ and ω. (Of course, the scale factor depends on the specified value of ω.) By further iterations in which ω is adjusted to correspond to a preassigned value of $\Delta\Omega^{\mathrm{f}}$, one obtains the parameters $(a, \lambda, \Sigma, \omega)$ that determine $\mathscr{C}^{\mathrm{f}}$ to within a scale factor, as well as that scale factor, from given data of the form $(\Delta\Omega^{\mathrm{f}}, \eta, \alpha, \beta)$ for a segment of length Λ^{f}. As, we observed in the text of the paper, our ability to do this calculation permits us to obtain the configuration $\mathscr{X}$ of $\mathscr{R}^{\mathrm{f}}$ as a function of $(\Lambda, w, h_0^{\mathrm{b}}, L_{\mathrm{k}})$. Moreover, in the course of calculating $\mathscr{X}$, we obtain $(a, \lambda, \Sigma, \omega)$ and ζ, and hence, by Eqs. A18, 10, and 12, the elastic energies Ψ^{f} and Ψ.

Remark about configurations corresponding to fixed geometric boundary data

To obtain insight into the nature of the dependence of the parameters $(a, \lambda, \Sigma, \omega)$ in Eq. A14 on the boundary data (η, α, β) for Eq. A2, we may temporarily ignore restrictions that arise when excluded volume is taken into account. Thus, for a given triple (η, α, β), we now consider the set $\mathscr{D}$ of all values of the quadruple $(a, \lambda, \Sigma, \omega)$ that are such that $P_3(u)$ has three real roots that give rise to a curve $\mathscr{C}^{\mathrm{f}}$ compatible with (η, α, β). It turns out that $\mathscr{D}$ is a collection $\mathscr{L}$ of closed curves in 4-space, each of which has a continuous parameterization of the form $(a(\sigma), \lambda(\sigma), \Sigma(\sigma), \omega(\sigma))$ with $0 \le \sigma < 2\pi$. For a curve ℓ in $\mathscr{L}$, let $W_{\mathrm{r}}(\sigma;\ell)$ be the writhe of the axial curve $\mathscr{C}$ of $\mathscr{R}$ when $\mathscr{R}^{\mathrm{f}}$ is in the configuration $\mathscr{X}$ determined by $(a(\sigma), \lambda(\sigma), \Sigma(\sigma), \omega(\sigma))$. Within the range of values of the parameters $(\Lambda, w, h_0^{\mathrm{b}}, L_{\mathrm{k}})$ that we have studied, precisely one curve ℓ^* in $\mathscr{L}$ has the property that for each of its points $(a, \lambda, \Sigma, \omega)$ the configuration corresponding to that point gives a value to the elastic energy Ψ of Eq. 10 that is smaller than the value of Ψ

for the configuration corresponding to any point on any other curve in the set $\mathcal{L}$. The function $\sigma \mapsto W_r(\sigma; \ell^*)$ is monotone and smooth, except at one point σ_J. At that point, W_r experiences a jump, $W_r(\sigma_J^+; \ell^*) - W_r(\sigma_J^-; \ell^*)$, of magnitude 2, because the parameters $(a(\sigma_J), \lambda(\sigma_J), \Sigma(\sigma_J), \omega(\sigma_J))$ yield an axial curve $\mathcal{C}^f$ that intersects and passes through itself. We choose the direction of increase of σ so that $W_r(\sigma; \ell^*)$ increases with σ on each interval that does not contain σ_J, and hence

$$W_r(\sigma_J^+; \ell^*) = W_r(\sigma_J^-; \ell^*) - 2. \tag{A27}$$

If we take the linking number L_k of $\mathcal{R}$ to be defined by Eq. 15 (so that it need not be an integer), then $L_k = L_k(\sigma; \ell^*)$ will be continuous in σ where $\sigma \neq \sigma_J$, and at σ_J will experience the same jump as W_r:

$$L_k(\sigma_J^+; \ell^*) = L_k(\sigma_J^-; \ell^*) - 2. \tag{A28}$$

Now, let Λ and w be compatible with (η, α, β), fix h_0^b, and let $I(\Lambda, w, h_0^b)$ be the open interval of values of L_k between $L_k(\sigma_J^+; \ell^*)$ and $L_k(\sigma_J^-; \ell^*)$. For each L_k in $I(\Lambda, w, h_0^b)$, the minimum value of Ψ in the class of all configurations compatible with (Λ, w, h_0^b, L_k), regardless of whether they are in equilibrium, is attained at $\mathcal{X}^*(\Lambda, w, h_0^b, L_k)$, the configuration determined by the unique point $(a, \lambda, \Sigma, \omega)$ on ℓ^* that corresponds to (Λ, w, h_0^b, L_k).

As the set $\mathcal{S}(N, w, h_0^b)$ defined in the text is a subset of the integers that are members of $I(\Lambda, w, h_0^b)$, the present remark explains why the calculations we have reported (which are restricted to cases in which self-contact does not occur) yield for $\mathcal{S}(N, w, h_0^b)$ a set with no more than two elements. Calculated values of W_r for elements L_k of $\mathcal{S}(N, w, h_0^b)$ at selected values of the triple (N, w, h_0^b) are shown in Fig. 4.

APPENDIX B: CALCULATION OF WRITHE

The writhe W_r and geometric torsion $\tau = \tau(s)$ of a closed curve $\mathcal{C}$ obey the following relation, which was obtained by Calugareanu (1961) and is discussed in papers of Pohl (1968) and White (1969):

$$W_r = S_k - \frac{1}{2\pi}\Theta, \qquad \Theta = \oint_{\mathcal{C}} \tau(s)\mathrm{d}s. \tag{B1}$$

Here S_k, the self-link, is an integer equal to the linking number of $\mathcal{C}$, with a closed curve $\mathcal{C}_\epsilon$ giving the locus of points that lie on the normal vectors $\boldsymbol{n}(s) = \kappa(s)^{-1}\,\boldsymbol{t}'(s)$ of $\mathcal{C}$ at an infinitesimal distance ϵ from $\mathcal{C}$. Hence W_r differs from $-(2\pi)^{-1}\Theta$ by an integer. Although S_k has several interesting geometric interpretations (see Pohl, 1968), no easily evaluated expression for that integer is known. Equation B1 is nonetheless valuable; if one evaluates the torsion integral Θ with precision and has in hand an approximate value of W_r, one can use Eq. B1 to first obtain the integer S_k and then the precise value of W_r. We shall show below that the explicit expression for $\mathbf{r}(s)$ obtained by the method explained in Appendix A permits us to derive an analytical formula for Θ, but first we present the approximation scheme we have used to determine a value of W_r that is sufficiently precise to fix the integer S_k.

As $\mathcal{C}$ is rectifiable, it can be arbitrarily closely approximated by a polygonal curve $\mathcal{C}_p$ for which the writhe W_r^p is given by an exact analytic expression. We take for $\mathcal{C}_p$ a polygon of M vertices, $\boldsymbol{r}_1 = \boldsymbol{r}(s_1)$, $\boldsymbol{r}_2 = \boldsymbol{r}(s_2)$, . . . , $\boldsymbol{r}_M = \boldsymbol{r}(s_M)$, that lie on $\mathcal{C}$ with $|s_i - s_{i-1}|$ independent of i. In the formulae that follow, we write $\boldsymbol{d}_{i-1}^{\,i}$ for the i'th segment $\boldsymbol{r}_i - \boldsymbol{r}_{i-1}$ (with $\boldsymbol{r}_0$ identified with $\boldsymbol{r}_M$) of $\mathcal{C}_p$; d_i for $|\boldsymbol{d}_{i-1}^{\,i}|$; and $\boldsymbol{d}_m^{\,k}$ for the vector $\boldsymbol{r}_k - \boldsymbol{r}_m$. We note that at each point of the interior of the i'th segment, the unit tangent vector for $\mathcal{C}_p$ (regarded as a curve) is $\boldsymbol{t}_i = \boldsymbol{d}_{i-1}^{\,i}/d_i$. In view of Eq. 4, the writhe W_r^p of $\mathcal{C}_p$ is

$$W_r^p = 2\sum_{i=1}^{M}\sum_{j=i+1}^{M} W_{ij}, \tag{B2}$$

where W_{ij} is the contribution to W_r^p from the segments $\boldsymbol{d}_{i-1}^{\,i}$ and $\boldsymbol{d}_{j-1}^{\,j}$:

$$W_{ij} = \frac{1}{4\pi}\int_0^{d_i}\int_0^{d_j} \frac{\boldsymbol{t}_i \times \boldsymbol{t}_j \cdot [(\boldsymbol{t}_i\sigma_i + \boldsymbol{r}_{i-1}) - (\boldsymbol{t}_j\sigma_j + \boldsymbol{r}_{j-1})]}{|(\boldsymbol{t}_i\sigma_i + \boldsymbol{r}_{i-1}) - (\boldsymbol{t}_j\sigma_j + \boldsymbol{r}_{j-1})|^3}\,\mathrm{d}\sigma_j\,\mathrm{d}\sigma_i. \tag{B3}$$

The double integral in Eq. B3 can be evaluated explicitly. To this end, let $\mu(\boldsymbol{t}_i, \boldsymbol{d}_m^{\,k}, \boldsymbol{t}_j)$ be the dihedral angle that the plane containing $\boldsymbol{t}_i$ and $\boldsymbol{d}_m^{\,k}$ makes with the plane containing $\boldsymbol{d}_m^{\,k}$ and $\boldsymbol{t}_j$, i.e.,

$$\cos\mu(\boldsymbol{t}_i, \boldsymbol{d}_m^{\,k}, \boldsymbol{t}_j) = \frac{[\boldsymbol{t}_i \times \boldsymbol{d}_m^{\,k}]\cdot[\boldsymbol{d}_m^{\,k} \times \boldsymbol{t}_j]}{|\boldsymbol{t}_i \times \boldsymbol{d}_m^{\,k}|\,|\boldsymbol{d}_m^{\,k} \times \boldsymbol{t}_j|}; \tag{B4}$$

μ is taken to be in the range $-\pi < \mu < \pi$, with a sign equal to that of $[\boldsymbol{t}_i \times \boldsymbol{t}_j] \cdot \boldsymbol{d}_m^{\,k}$. After some calculation we have found that Eq. B3 is equivalent to

$$W_{ij} = \frac{1}{4\pi}[\mu(\boldsymbol{t}_i, \boldsymbol{d}_{j-1}^{\,i-1}, \boldsymbol{t}_j) - \mu(\boldsymbol{t}_i, \boldsymbol{d}_{j-1}^{\,i}, \boldsymbol{t}_j) - \mu(\boldsymbol{t}_i, \boldsymbol{d}_j^{\,i-1}, \boldsymbol{t}_j) + \mu(\boldsymbol{t}_i, \boldsymbol{d}_j^{\,i}, \boldsymbol{t}_j)]. \tag{B5}$$

(The equivalence can be verified by differentiating $\mu(\boldsymbol{t}_i, \boldsymbol{d}_{j-1}^{\,i-1} + \boldsymbol{t}_i\sigma_i - \boldsymbol{t}_j\sigma_j, \boldsymbol{t}_j)$ with respect to σ_i and σ_j, and using Eq. B4.)

If $\mathcal{C}$ is the duplex axis of a mononucleosomal minicircle of the type discussed in this paper, Θ is given by the exact expressions derived below, and, once W_r^p is calculated from Eqs. B2 and B5, S_k for insertion in Eq. B1 can be obtained by rounding off $W_r^p + (2\pi)^{-1}\Theta$ to the nearest integer. When we compare the precise value of W_r so obtained with W_r^p, we find that if $M = 200$, W_r^p is equal to W_r up to three significant figures. Thus the approximation to W_r given by Eqs. B2 and B5 can be a very good one and is expected to be useful, even for curves for which the application of Eq. B1 is not feasible, because of difficulties in evaluating the torsion integral Θ. In cases such as the present one, in which Θ is known, for use of Eq. B1 to obtain S_k it suffices to know W_r to within an error of ± 0.4, and hence smaller values of M can be employed.

For the mononucleosome,

$$\Theta = \int_{\mathcal{C}^b} \tau(s)\mathrm{d}s + \int_{\mathcal{C}^f} \tau(s)\mathrm{d}s + \xi_A + \xi_B; \tag{B6}$$

for $I = A$ or B, ξ_I is the dihedral angle that the osculating plane at s_I^+ makes with the osculating plane at s_I^- when s_I is a boundary point of $\mathcal{C}^b$, i.e.,

$$\xi_I = \lim_{\epsilon\to 0}\int_{s_I-\epsilon}^{s_I+\epsilon} \tau(s)\mathrm{d}s = \lim_{\epsilon\to 0}\cos^{-1}(\boldsymbol{b}(s_I - \epsilon)\cdot\boldsymbol{b}(s_I + \epsilon)), \tag{B7}$$

where $\boldsymbol{b} = \boldsymbol{t} \times \boldsymbol{n}$, and the sign of ξ_I is equal to that of $\lim_{\epsilon\to 0}\boldsymbol{b}(s_I - \epsilon)\cdot\boldsymbol{n}(s_I + \epsilon)$. Symmetry here yields $\xi_A = \xi_B$. For the helix $\mathcal{C}^b$, τ, in conventional units, is the constant,

$$\tau^b = \frac{-2\pi p}{\pi^2 d^2 + p^2}, \tag{B8}$$

i.e.,

$$\int_{\mathcal{C}^b} \tau(s)\mathrm{d}s = \Lambda^b\tau^b = \frac{-2\pi w p}{\sqrt{\pi^2 d^2 + p^2}}. \tag{B9}$$

For the free segment $\mathcal{R}^f$, Eqs. A7, A8, A9, and A12 yield, in dimensionless units,

$$\tau(s) = \frac{\omega}{2} - \frac{4\lambda + (1/2)\omega^3 - 2\omega(\lambda^2 + a)}{4(u_3 + \lambda^2) - \omega^2 - 4(u_3 - u_2)\mathrm{sn}^2(s\sqrt{u_3 - u_1})}, \tag{B10}$$

from which one can obtain the following relation (which is independent of the unit of length):

$$\int_{\mathcal{C}^f} \tau(s)\mathrm{d}s = \frac{\Sigma\omega}{2} - \frac{4\lambda + (1/2)\omega^3 - 2\omega(\lambda^2 + a)}{[4(u_3 + \lambda^2) - \omega^2]\sqrt{u_3 - u_1}}\, 2\Pi(\tilde{n}; \psi^f|m), \tag{B11}$$

where

$$\tilde{n} = \frac{u_3 - u_2}{u_3 + \lambda^2 - (1/4)\omega^2}, \qquad \frac{\Sigma}{2} = \frac{\mathrm{F}(\psi^f|m)}{\sqrt{u_3 - u_1}}; \tag{B12}$$

m, u_i, Σ, etc., are as in Appendix A, and F and Π are the elliptic integrals defined in Eqs. A15 and A17. Equations B6–B12 give an essentially explicit expression for the torsion integral of the duplex axis of a DNA minicircle in a mononucleosome.

This research was supported by the National Science Foundation under grant DMS-8-04580 and the United States Public Health Service under grant GM34809, David Swigon acknowledges support by a Fellowship from the Program in Mathematics and Molecular Biology at the Florida State University with funding from the Burroughs Wellcome Fund Interfaces Program. This paper was a research contribution presented at the DIMACS/MBBC/PMMB Workshop on DNA Topology, Rutgers University, April 1997.

REFERENCES

Arents, G., and E. N. Moudrianakis. 1993. Topography of the histone octamer surface: repeating structural motifs utilized in the docking of nucleosomal DNA. *Proc. Natl. Acad. Sci. USA.* 90:10489–10493.

Calugareanu, G. 1961. Sur les classes d'isotopie des noeuds tridimensionnels et leurs invariants. *Czech. Math. J.* 11:588–625.

Coleman, B. D., E. H. Dill, M. Lembo, Z. Lu, and I. Tobias. 1993. On the dynamics of rods in the theory of Kirchhoff and Clebsch. *Arch. Rat. Mech. Anal.* 121:339–359.

Coleman, B. D., I. Tobias, and D. Swigon. 1995. Theory of the influence of end conditions on self-contact in DNA loops. *J. Chem. Phys.* 103: 9101–9109.

Courant, R. 1936. Differential and Integral Calculus, Vol. II, English Ed. Blackie, London. 410–411.

Dill, E. H. 1992. Kirchhoff's theory of rods. *Arch. Hist. Exact. Sci.* 44: 1–23.

Felsenfeld, G. 1996. Chromatin unfolds. *Cell.* 86:13–19.

Fuller, F. B. 1971. The writhing number of a space curve. *Proc. Natl. Acad. Sci. USA.* 68:815–819.

Goulet, I., Y. Zivanovic, A. Prunell, and B. Revet. 1988. Chromatin reconstitution on small DNA rings. I. Supercoiling on the nucleosome. *J. Mol. Biol.* 200:253–266.

Hagerman, P. J. 1988. Flexibility of DNA. *Annu. Rev. Biophys. Biophys. Chem.* 17:265–286.

Hamiche, A., and A. Prunell. 1992. Chromatin reconstitution on small DNA rings. V. DNA thermal flexibility of single nucleosomes. *J. Mol. Biol.* 228:327–337.

Hayes, J. J., D. J. Clark, and A. P. Wolffe. 1991. Histone contributions to the structure of DNA in the nucleosome. *Proc. Natl. Acad. Sci. USA.* 88:6829–6833.

Hayes, J. J., T. D. Tullius, and A. P. Wolffe. 1990. The structure of DNA in a nucleosome. *Proc. Natl. Acad. Sci. USA.* 87:7405–7409.

Horowitz, D. S., and J. C. Wang. 1984. Torsional rigidity of DNA and length dependence of the free energy of DNA supercoiling. *J. Mol. Biol.* 173:75–91.

Katritch, V., and A. Vologodskii. 1997. The effect of intrinsic curvature on conformational properties of circular DNA. *Biophys. J.* 72:1070–1079.

Kirchhoff, G. 1859. Über das Gleichgewicht und die Bewegung eines unendlich dünnen elastischen Stabes. *J. F. Reine Angew. Math.* 56: 285–313.

Kirchhoff, G. 1876. Vorlesungen über Mathematische Physik, Mechanik, Vorlesung 28. Tuebner, Leipzig.

Landau, L. D., and E. M. Lifshitz. 1986. Theory of Elasticity, 3rd Ed. Pergamon, Oxford.

Le Bret, M. 1988. Computation of the helical twist of nucleosomal DNA. *J. Mol. Biol.* 200:285–290.

Luger, K., A. W. Mäder, R. K. Richmond, D. F. Sargent, and T. J. Richmond. 1997. Crystal structure of the nucleosome core particle at 2.8 Å resolution. *Nature.* 389:251–260.

Lutter, L. C. 1979. Precise location of DNase I cutting sites in the nucleosome core determined by high resolution gel electrophoresis. *Nucleic Acids Res.* 6:41–56.

Pohl, W. F. 1968. The self-linking number of a closed space curve. *J. Math. Mech.* 17:975–985.

Polach, K. J., and J. Widom. 1995. Mechanism of protein access to specific DNA sequences in chromatin: a dynamic equilibrium model for gene regulation. *J. Mol. Biol.* 254:130–149.

Polach, K. J., and J. Widom. 1996. A model for the cooperative binding of eukaryotic regulatory proteins to nucleosomal target sites. *J. Mol. Biol.* 258:800–812.

Prunell, A. 1983. Periodicity of exonuclease III digestion of chromatin and the pitch of deoxyribonucleic acid on the nucleosome. *Biochemistry.* 22:4887–4894.

Prunell, A., R. D. Kornberg, L. C. Lutter, A. Klug, M. Levitt, and F. H. Crick. 1979. Periodicity of deoxyribonuclease I digestion of chromatin. *Science.* 204:855–858.

Richmond, T. J., J. T. Finch, B. Rushton, D. Rhodes, and A. Klug. 1984. Structure of the nucleosome core particle at 7 Å resolution. *Nature.* 311:532–537.

Shore, D. and R. L. Baldwin. 1983. Energetics of DNA twisting. II. Topoisomer analysis. *J. Mol. Biol.* 170:983–1007.

Sutcliffe, J. G. 1978. pBR322 restriction map derived from the DNA sequence: accurate DNA size markers up to 4361 nucleotide pairs long. *Nucleic Acids Res.* 5:2721–2728.

Sutcliffe, J. G. 1979. Complete nucleotide sequence of the *Escherichia coli* plasmid pBR322. *Cold Spring Harb. Symp. Quant. Biol.* 43:77–90.

Tobias, I. 1998. A theory of thermal fluctuations in DNA miniplasmids. *Biophys. J.* 74:2545–2553.

Tobias, I., B. D. Coleman, and W. Olson. 1994. The dependence of DNA tertiary structure on end conditions: theory and implications for topological transitions. *J. Chem. Phys.* 103:10990–10996.

Watson, N. 1988. A new revision of the sequence of plasmid pBR322. *Gene.* 70:399–403.

White, J. H. 1969. Self-linking and the Gauss integral in higher dimensions. *Am. J. Math.* 91:693–728.

Zhang, P., I. Tobias, and W. Olson. 1994. Computer simulation of protein-induced structural changes in closed circular DNA. *J. Mol. Biol.* 242: 271–290.

Zivanovic, Y., I. Goulet, B. Revet, M. LeBret, and A. Prunell. 1988. Chromatin reconstitution on small DNA rings. II. Supercoiling on the nucleosome. *J. Mol. Biol.* 200:267–285.